CNIC-01680
CNDC-0034
INDC(CPR)-058/L

COMMUNICATION OF NUCLEAR DATA PROGRESS

No. 27 (2002. 6)

China Nuclear Data Center
China Nuclear Information Centre
China Nuclear Industry Audio & Visual Publishing House

COMMUNICATION OF NUCLEAR DATA PROGRESS

EDITORIAL NOTE

The editors hope that our readers and colleagues will not spare their comments in order to improve this publication. If you have any, please contact us by following address:

Mailing Address: Profs. LIU Tingjin and ZHUANG Youxiang
China Nuclear Data Center
China Institute of Atomic Energy
P.O. Box 275 (41), Beijing 102413
People's Republic of China
Telephone: 86-10-69357729 or 69357830
Facsimile: 86-10-6935 7008
E-mail: tjliu @ iris.ciae.ac.cn or yxzhuang @ iris.ciae.ac.cn

Abstract: This is the 27th issue of *Communication of Nuclear Data Progress* (CNDP), in which the achievements in nuclear data field for the last year in China are carried. It includes the measurements of ^{6}Li(n,t)^{4}He differential cross section at 1.85, 2.67 MeV, and ^{197}Au(n,2n)^{196m2}Au reaction cross sections at around 14 MeV, theoretical calculations of n+$^{112, 120}$Sn cross section and spectra, BAR-MOM code and its application, a testing of RIPL with UNF code calculation in energy region 0.1~20 MeV, and the comparison of two level density models calculation in energy region 0~20 MeV; evaluations of prompt and delayed neutron yields for ^{239}Pu, ^{197}Au(n,2n)^{196}Au cross section, the effect of the decay data on activation cross section. Also the activities and cooperation on nuclear data in China are summarized.

Communication of Nuclear Data Progress

No.27 (2002) Beijing

CONTENTS

218 Differential Cross Section Measurement for the $^{6}Li(n,t)^{4}He$ Reaction
ZHANG Guohui et al.

221 Measurement of Isomer Cross Section for the $^{197}Au(n,2n)^{196m2}Au$ Reaction at around 14 MeV
MOU Yunfeng et al.

224 BAR-MOM Code and Its Application
WANG Shunuan

226 Calculations of $n+^{112,120}Sn$ Reactions in the Energy Region up to 20 MeV
DUAN Junfeng et al.

231 Evaluation of Prompt and Delayed Neutron Yields for ^{239}Pu from 10^{-5} eV to 20 MeV
YU Baosheng et al.

236 The Cross Section Evaluation and Recommendation of $^{197}Au(n,2n)^{196}Au$ Reaction
FAN Sheng et al.

241 The Effect of the Decay Data on Activation Cross Section
HUANG Xiaolong

244 A Testing of RIPL with UNF Code Calculation in Energy Region 0.1~20 MeV
GE Zhigang et al.

247 A Comparison of Two Level Density Models in Energy Region 0~20 MeV
GE Zhigang

250 Activities and Cooperation in Nuclear Data Field in China during 2001
ZHUANG Youxiang

251 **CINDA INDEX**

Differential Cross Section Measurement for the $^{6}Li(n,t)^{4}He$ Reaction

ZHANG Guohui TANG Guoyou CHEN Jinxiang SHI Zhaomin
Institute of Heavy Ion Physics & MOE Key Laboratory of Heavy Ion Physics, Peking University, Beijing 100871

CHEN Zemin
Department of Physics, Tsinghua University, Beijing 100084

Yu. M. Gledenov M. Sedysheva G. Khuukhenkhuu
Joint Institute for Nuclear Research, Frank Laboratory of Neutron Physics, Dubna 141980, Russia

【abstract】 *The differential cross sections and integrated cross sections of the $^{6}Li(n,t)^{4}He$ reaction were measured at 1.85 and 2.67 MeV by using a gridded ionization chamber. Neutrons were produced through the $T(p,n)^{3}He$ reaction. The absolute neutron flux was determined through the $^{238}U(n,f)$ reaction. Present results are compared with existing data.*

Introduction

The differential cross section data and cross section data of the $^{6}Li(n,t)^{4}He$ reaction are important in practical applications as well as for the study of reaction mechanisms. There are a few existing differential cross section data in the MeV neutron energy region, but there are large discrepancies among them[1~6].

In our previous work, measurement of differential cross section data for the $^{6}Li(n,t)^{4}He$ reaction were carried out at 3.67 and 4.42 MeV by using the gridded ionization chamber (GIC) [7]. In the present experiment, we extend our study to 1.85 and 2.67 MeV.

1 Details of Experiment

The experiment was performed at the 4.5 MV Van de Graaff accelerator of the Institute of Heavy Ion Physics, Peking University. Mono-energetic neutrons were produced through the $T(p,n)^{3}He$ reaction with a T-Ti target of 1.30 mg/cm^2 in thickness. The energies of the beams of protons before entering the target were 2.70 and 3.50 MeV, and by Monte Carlo calculation, the corresponding neutron energies were 1.85±0.05 and 2.67±0.04 MeV.

The structure of the gridded ionization chamber and the electronics were described in Ref [7]. For the present experiment, the working gas was Kr+2.73CO_2. The distances from the cathode to the grid, the grid to the anode and the anode to the shield are 4.3, 2.2 and 1.1 cm, respectively. The thermal cross section of the $^{6}Li(n,t)^{4}He$ reaction is as large as 936 b, and this is a strong interference to the measured events. In order to reduce this interference, the ionization chamber was coated with a layer of cadmium ~0.5 mm in thickness.

The sample material was ^{6}LiF with the ^{6}Li abundance of 91.24%. It was evaporated on a tungsten backing. The area and thickness of the sample were 15.90 cm^2 and 228.3 μg/cm^2, respectively. Apart from the ^{6}LiF sample, there was a tungsten sheet set on the sample changer of the GIC for background measurement. A ^{238}U fission foil (99.999% in purity, 7.85±0.10 mg in weight, 4.50 cm in diameter) is also set on the sample changer for absolute neutron flux measurement. A compound α source was placed on the other position of the sample changer for the energy calibration of the data acquisition system.

Only the front side of the GIC and the corresponding electronics were used in the present measurement due to the interference from thermal neutron induced events. Although the *Q* value of the $^{6}Li(n,t)^{4}He$ reaction is as large as 4.786 MeV, the backward (90°~180°) events could not be separated from thermal neutron induced events because of the

kinematical effect. Therefore, triton data in backward angles were obtained by measuring the forward (0°~90°) α events because in the center-of-mass system, one triton event corresponds to one α event in opposite direction. Fig.1 is the two-dimensional spectrum for forward α measurement at E_n=2.67 MeV, from which the kinematical effect can be seen.

For α measurement, the pressure of the working gas of the GIC was 6.08×10^4 Pa (0.60 atm) and 4.76×10^4 Pa (0.47 atm) for 1.85 and 2.67 MeV measurement, respectively. The voltages for cathode, grid and anode were −700, 0 and 600 V, respectively, for the above two energy points. For triton measurement, the gas pressure was 3.34×10^5 Pa (3.30 atm) and the voltages were −3300, 0 and 2600 V for the two energy points.

Fig.2 shows the two-dimensional spectrum for forward triton measurement (E_n=1.85 MeV). As seen in this figure, triton events in large angles (near 90°) overlap with α events but the interference is only confined in the region near 90° line. For α measurement there was no such problem because the triton energy loss in the sensitivity volume is very small compared to α energy due to the low gas pressure.

A BF_3 long counter, placed at 0° relative to the beam line and at the distance of 3.0 m from the T-Ti target, was used as neutron flux monitor. The cross section data of the ^{238}U(n,f) reactions were taken from the ENDF/B-6 library.

The deuteron beam current was ~3.0 μA during the experiment. The center of the chamber was placed at 0° relative to the beam line, and the distance from its cathode to the neutron source was 38.0 cm. The duration for α or triton events plus background measurement was about 9 h, and for the pure background measurement and the absolute neutron flux calibration were both about 4 h.

2 Results

Fig. 3 and Fig. 4 show the measured differential cross sections transferred to the center-of-mass system at 1.85 and 2.67 MeV, respectively. Present differential cross sections are compared with existing data [1~6]. Our differential data are listed in Table 1. Backward triton data were obtained by translating the forward α data as described above. In dealing with forward triton or α data, the region near the 90^0 line ($\cos\theta_L$=0~0.3) were excluded because of α interference and the absorption effect in the sample. Principal sources of error and their magnitudes for the measured differential cross-section data are listed in Table 2.

Table 1 Differential cross-section data of tritons in the c.m. system for the ^{6}Li(n,t)^{4}He reaction

E_n=1.85 MeV		E_n=2.67 MeV	
$\cos\theta_c$	$d\sigma/d\Omega$ (mb/sr)	$\cos\theta_c$	$d\sigma/d\Omega$ (mb/sr)
–0.925	14.40 ± 0.99	–0.921	9.21 ± 0.65
–0.778	15.17 ± 0.78	–0.767	10.72 ± 0.57
–0.638	15.78 ± 0.81	–0.621	12.36 ± 0.65
–0.504	17.04 ± 0.87	–0.481	13.67 ± 0.71
–0.375	17.22 ± 0.89	–0.349	12.94 ± 0.68
–0.252	19.73 ± 1.00	–0.223	14.01 ± 0.73
–0.135	17.92 ± 1.24	–0.103	14.12 ± 0.98
0.190	23.18 ± 1.70	0.166	15.52 ± 1.12
0.303	21.52 ± 1.16	0.281	19.23 ± 1.05
0.420	21.15 ± 1.13	0.401	19.34 ± 1.06
0.542	20.19 ± 1.08	0.526	17.99 ± 0.98
0.667	18.65 ± 1.00	0.655	14.86 ± 0.82
0.797	19.30 ± 1.03	0.789	12.48 ± 0.72
0.931	17.47 ± 1.24	0.928	9.40 ± 0.69

Table 2 Principal sources of error and their magnitudes for the measured differential cross section data

Source of uncertainty	Relative error (%)
^{238}U(n,f) cross section	1.3~2.9
Determination for the number of fission counts	2.2~3.5
Statistics for α or t counts	2.2~3.3
Normalization in background subtraction and neutron flux determination	2.0~5.0
Atom number of ^{238}U in the fission foil	1.2
Atom number of ^{6}Li in the ^{6}LiF sample	0.5
Total	5.1~7.3

Angle integrated cross-sections for the ^{6}Li(n,t)^{4}He reaction were derived from the differential data via Legendge polynomial fitting. The cross sections are 233.6±13.8 mb and 174.5±10.3 mb at 1.85 and 2.67 MeV, respectively. In Fig. 5, present results are compared with existing data [8~12].

Acknowledgement

The authors are indebted to the China Nuclear Data Center for financial support. Thanks are also given to the crew of 4.5 MV Van de Graaff of Peking University.

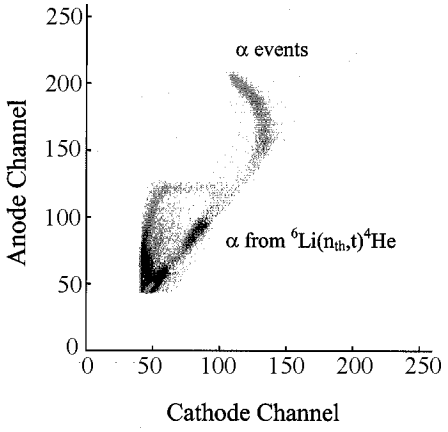

Fig.1 The two-dimensional spectrum for forward α measurement at E_n=2.67 MeV

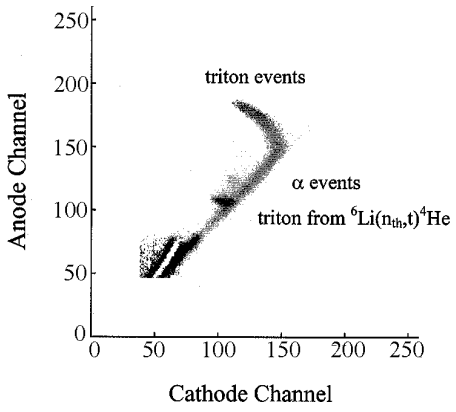

Fig.2 The two-dimensional spectrum for forward triton measurement at E_n=1.85 MeV

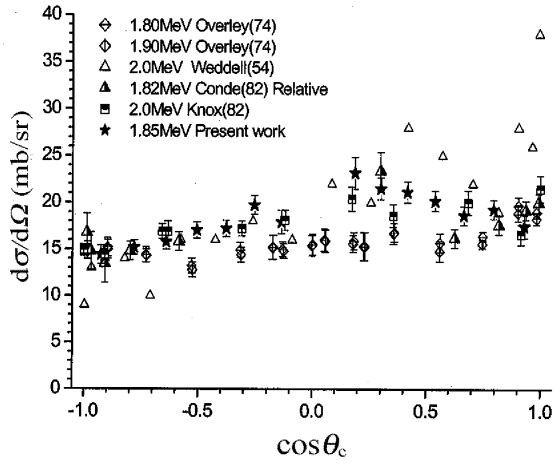

Fig.3 Differential cross sections in the c.m. system for the ^{6}Li(n,t)^{4}He reaction at 1.85 MeV compared with existing data

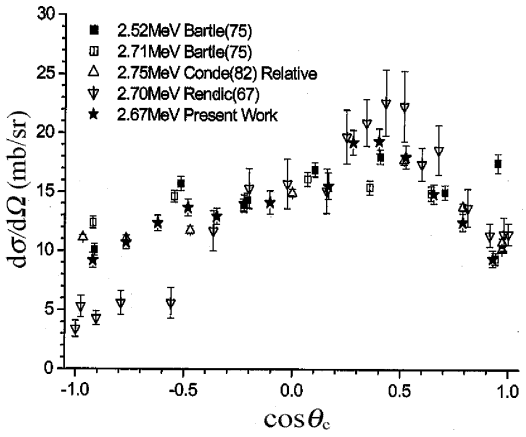

Fig.4 Differential cross section in the c.m. system for the ^{6}Li(n,t)^{4}He reaction at 2.67 MeV compared with existing data

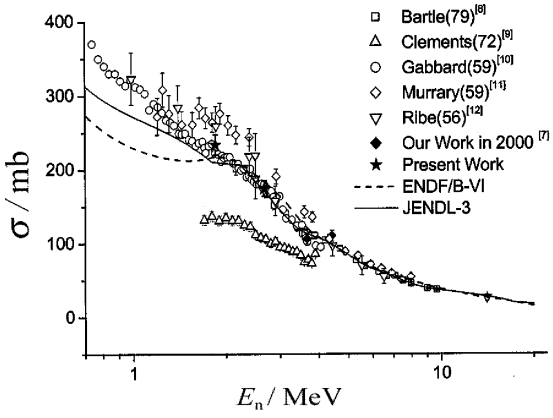

Fig. 5 The present result of the ^{6}Li(n,t)^{4}He reaction cross section compared with existing data

References

[1] J. C. Overlay, et al. NP/A 221,573 (1974).
[2] J. B. Weddell, et al. PR, 95,117 (1954)
[3] H. Conde, et al. 82ANTWER, 447, 1982.
[4] H.G. Knox. BAP, 27, 703(DE12) (1982).
[5] C.M. Bartle, et al. 75WASH, 688, 1975.
[6] D. Rendic, et al. ZFK-130, 143, 1967; NP/A, 98, 305 (1967).
[7] G. Zhang, et al. Nucl. Sci. Eng., 134, 312 (2000).
[8] C. M. Bartle. Nucl. Phys., A 330, 1 (1979).
[9] P. J. Clements, et al. EANDC(UK)-141, 1972.
[10] F. Gabbard, et al. Phys. Rev., 114, 201 (1959).
[11] R. B. Murry, et al. Phys. Rev., 115, 1707 (1959).
[12] F. L. Ribe. Phys. Rev., 103, 741 (1956).

Measurement of Isomer Cross Section for the ^{197}Au(n,2n)^{196m2}Au Reaction at around 14 MeV

MOU Yunfeng[1,2] LIN Libin[1] CHEN Yuan[2] GUO Haiping[2] AN Li[2] WANG Xinhua[2] CHEN Yinliang[2]

1 Physics Department of Sichuan University, Key Laboratory of Education Ministry on Radiation Physics and Technology, 610000

2 Southwest Institute of Nuclear Physics and Chemistry, Mianyang, Sichuan, 621900)

【abstract】 *The intensity of ^{196m2}Au 148 keV γ-ray and time relation of intensity of ^{196g}Au 356 keV γ-ray were measured with a HPGe detector. The cross section of ^{197}Au(n,2n)^{196m2}Au was obtained to be 182±15mb, by two methods with DT neutrons.*

Introduction

There are 9 sets of experimental data for ^{197}Au(n,2n)^{196m2}Au reaction at around 14 MeV, in EXFOR library, but their values of the cross sections range from 128 to 230 mb[2~10], and 152 mb was adopted in ENDF/B-6. However, in 1999 F. Maekawa et al. at JAERI found that the cross section of ^{197}Au(n,2n) ^{196m2}Au reaction in both JENDL and FENDL was too small, their experiment indicated that this cross section should be near 200 mb[1]. In Previous work some other activation foil of standard cross section was used as monitor to measure the cross section of ^{197}Au(n,2n)^{196m2}Au reaction. In this work the intensity of time relation of ^{196g}Au 356 keV γ-ray was measured to obtain isomer ratio of ^{197}Au(n,2n)^{196m2,g}Au reaction. The intensity of the ^{196m2}Au 148 keV γ-ray was also measured to get the cross section for ^{197}Au(n,2n) ^{196m2}Au reaction for comparison.

1 Principle

There are 3 products in ^{197}Au(n,2n)^{196}Au reaction: ^{196g}Au ($T_{1/2}$=6.182 d), ^{196m1}Au ($T_{1/2}$=8.1 s), and ^{196m2}Au ($T_{1/2}$=9.7 h) . Both ^{196m1}Au directly and ^{196m2}Au decay in cascade in ^{196g}Au are shown in Fig.1.

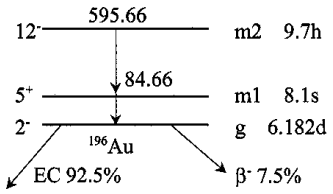

Fig.1 ^{196}Au isomer decay

When ^{196m2}Au decays, it gives out γ-rays of 147.73 keV(37.0%) and 188 keV(32.6%). While ^{196g}Au decays, it emits γ-rays of 333 keV(22.6%) and 355.7 keV(86.6%). Since ^{196m1}Au is so short-lived, it can be grouped into ^{196g}Au. Assuming the cross-section of ^{197}Au(n, 2n) ^{196}Au is σ, and the cross-section of ^{197}Au(n,2n) $^{196m1+g}$Au and ^{197}Au(n,2n) ^{196m2}Au are σ_1 and σ_2 respectively. Supposing nuclear numbers of ^{197}Au, $^{196g+m1}$Au and ^{196m2}Au are N, N_1 and N_2 respectively, and neutron flux is I at the location of activation foil during the process of radiation,

$$\frac{dN_1(t)}{dt} = NI\sigma_1 + \lambda_2 N_2 - \lambda_1 N_1 \quad (1)$$

$$\frac{dN_2(t)}{dt} = NI\sigma_2 - \lambda_2 N_2 \quad (2)$$

with the initial condition $N_1(t=0)=0$, $N_2(t=0)=0$. Where t and λ stand for time (in second) and decay constant. Solving the above equations, we get

$$N_1 = \frac{NI\sigma}{\lambda_1}(1-e^{-\lambda_1 t}) + \frac{NI\sigma_2}{\lambda_1-\lambda_2}(e^{-\lambda_1 t} - e^{-\lambda_2 t}) \quad (3)$$

$$N_2 = \frac{NI\sigma_2}{\lambda_2}(1-e^{-\lambda_2 t}) \quad (4)$$

If the radiation time t_0 is very short (i.e. $\lambda_1 t_0 << 1$ and $\lambda_2 t_0 << 1$), the nuclear numbers of $^{196m1+g}$Au and ^{196m2}Au are $N_{10}=IN\sigma_1 t_0$, $N_{20}=IN\sigma_2 t_0$ respectively.

In decay process of the activated sample

$$\frac{dN_1(t)}{dt} = \lambda_2 N_2 - \lambda_1 N_1 \quad (5)$$

$$\frac{dN_2(t)}{dt} = -\lambda_2 N_2 \quad (6)$$

Solve the above equations, we get

$$N_1(t) = (N_{10} - \frac{\lambda_2}{\lambda_1 - \lambda_2} N_{20})e^{-\lambda_1 t} - \frac{\lambda_2}{\lambda_1 - \lambda_2} N_{20} e^{-\lambda_2 t} \quad (7)$$

$$\approx NI\sigma\ t_0 e^{-\lambda_1 t}(1 - 1.07\frac{\sigma_2}{\sigma} e^{(\lambda_1 - \lambda_2)t})$$

$$N_2(t) = N_{20} e^{-\lambda_2 t} \quad (8)$$

The cross section ratio of σ_2/σ could be obtained through Eq. (7), if the activity of ^{196g}Au is measured. The counting-rates of 356 keV and 148 keV peaks are as follow

$$n_2 = a_2 b_2 \varepsilon_2 \lambda_2 N_2 \quad (9)$$

$$n_1 = a_1 b_1 \varepsilon_1 \lambda_1 N_1 = f(e^{-\lambda_1 t} - 1.07\frac{\sigma_2}{\sigma} e^{-\lambda_2 t}) \quad (10)$$

where a, b, ε stand for self-absorption of γ-ray, branch ratio, and peak efficiency of the HPGe detector to corresponding γ-ray respectively; f is the factor introduced only for simplification.

According to what mentioned above, we have two ways to get σ_2/σ. One is to directly compare the count-rates of both ^{196g}Au 356 keV γ-ray and ^{196m2}Au 148 keV γ-ray. Another is through the relationship of count rate and time (n_1~t) for 356 keV γ-ray of ^{196g}Au, to determine σ_2/σ value indirectly. Using the second way, two sets of data (t,n_1) are needed to get σ_2/σ.

2 Experiment

The gold foils are in size of Φ16 mm×0.2 mm，with a purity less than 99.9%。During radiation, the foil was put closing to the shell of the target chamber. Two foils were used. One (No.1) was set at 120° direction, so the energy of the neutrons through the foil was 13.75±0.3 MeV. This foil was radiated for 1 hour, until the integrated neutron flux from the T-Ti target reached to 1×10^{14}/s. The other was radiated for only 15 min, in a position where the neutron energy was 14.1±0.2 MeV with lower neutron flux.

The intensities of γ-rays from the foils were measured with a closed-end co-axial HPGe detector with a value of Φ58 mm×63 mm. There was an Al capsule of 1 mm thick, 3 mm away from the surface of Ge crystal. The samples were measured in 2 positions on the axis: position A-at the center of the capsule; position B-84 mm away from the capsule.

2.1 Indirect Method

At each position, the foils were measured more than twice, and 2 sets of data of (t,n_1) were used to get σ_2/σ (see Table 1). The counting-rate of 356 keV γ-ray for ^{196g}Au of No.2 sample at position B was shown in Fig. 2 (dot with error-bars). A function with 2 exponential parameter was used to fit the data, and

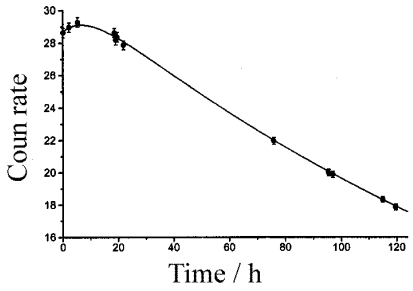

Fig. 2 The relationship between connt ralt and time for 356 keV γ-ray of ^{196g}Au

it indicated the relationship between time and counting-rate.

2.2 Direct Method

The No.2 foil was measured in position B. The counting-rates of ^{196m2}Au 148 keV and ^{196g}Au 356 keV peaks are given in Table 2 together with necessary parameters and the present results.

The peak efficiency of the detector and self-absorption of γ-rays from the gold sample were obtained in another experiment.

3 Discussion

The 197Au(n,2n)196Au cross-section was taken as a standard. Therefor the measured reaction and monitor reaction have the same neutron flux and same nuclear number of target. The direct method to determine σ_2/σ by ^{196m2}Au 148 keV γ-ray and 196gAu 356 keV γ-ray is slightly different from the way used in the previous work.

The indirect method, by which σ_2/σ was determined by the dependence of counting-rate on time, would be more reliable, because such factors as efficiency, branch-ratio and self-absorption of the sample need not to be considered.

The statistics errors of the counting-rates were within 2%. Since there were less factors in the indirect method, it may be more reliable. But there is disadvantage in this method. A slight shift of measured position may bring a great change in result. Due to this, the result of No.1 sample in position A was rejected.

^{196m2}Au 148 keV γ-ray decays with a $T_{1/2,2}$ of 9.7 h. But it was found that $T_{1/2,2}$ obtained from the curve in Fig. 2 was 6.0 h instead of 9.7 h. The reason is not clear at present.

Four σ_2/σ results were obtained. They are 0.089, 0.082, and 0.078 from indirect method and 0.095 from direct method. In common sense, the

Table 1 Indirect measurement

Experimental data					
No.1（13.75MeV）		No.2（14.1MeV）			
Position B		Position A		Position B	
Cool-tme/h	Count-rate	Cool-time /h	Count-rate	Cool-time /h	Count-rate
5.8	26.93±0.15	0.08	28.6±0.3	1.0	2.37±.04
310.8	6.93±0.06	115	18.3±0.2	95.5	1.65±.02
Results					
σ_2/σ	0.089	0.082		0.078	
σ_2 / mb	187	175		164	

Table 2 Direct measurement

		^{196m2}Au 148 keV	^{196g}Au 356 keV
measured	Cool-time/h	1.0	96.0
	Peak count-rate	1.60±0.03	1.45±0.03
parameter	Peak efficiency	0.0117	0.0073
	Self-absorption	0.741	0.963
	branch	0.37	0.87
results			
	σ_2/σ=0.095	σ=200 mb	

cross-section would change smoothly and slowly with energy, so the results should be nearly the same. After treatment, σ_2/σ=0.086±0.007. σ=2.12 b was taken from ENDF/B-6, σ_2=182±15 mb is obtained in present work. This result is 20% higher than activation cross-section in ENDF/B-6, but is close to that of literature[1].

4 Conclusion

The isomer ratio σ_2/σ of ^{197}Au(n,2n)^{196m2,g}Au were measured with two methods; it is 0.086±0.007; and taken the ^{197}Au(n,2n)^{196}Au cross-section of ENDF/B-6 as standard, the cross section of ^{197}Au(n,2n) ^{196m2}Au is 182±15 mb.

Reference

[1] F. Maekawa，Ulrich von Mollendorff,，P.H.Wilson and Y. Ikeda. “Determination of a Deuteron-Beryllium Neutron Source Spectrum by Multifoil Activation”, FUSION TECHNOLGY Vol. 36 P165-172, sept. 1999.

[2] A.K.Hankla, R.W.Fink and J.H.Hamilton, “Neutron Activation Cross Section at 14.4MeV for Some Naturally Occurring Heavy Elements in the Region z=76-82”, J, NP/A,180,157,1972.

[3] H. A.Tewes,A.A.Caretto,A.E.Miller and D.R.Nethaway, “Excitation Functions of Neutron-Induced Reactions”, R, UCRL-6028-T, 1960.

[4] R.J.Prestwood,B.P.Bayhurst, “(n,2n) Excitation Functions of Several Nuclei from 12.0 to 19.8 MeV”, J, PR, 121,1438,1961.

[5] P.C.Harper, W.L.Alford, “Experimental and Theoretical Neutron Cross Sections at 14MeV”, J,JP/G,8,153,1982.

[6] S. K. Ghorai, K. C. Hayworth, J. R. Williams, W.L.Alford, “Isomeric Yield Ratios and Isomeric Cross Section for the Au-197(n,2n) Reaction”, J,BAP, 29, (P2.100),1117,1984.

[7] W. Dilg, H. Vongch, G. Winkler, P. Hille, J, NP/A, 118, 9, 1968.

[8] J.Laurec , A.Adam, T. de Bruyne, “-Measurement of the (n,2n) Reaction Cross Sections of the Nuclei Y-89, Rh-103,Ag-107, Tm-169, Lu-175 and Au-197 at 14.1 and 14.8MeV-(in French)”, R, CEA-R-5109, 1981

[9] YANG Weifan, LI Yingjun, YU Jusheng, ZHAO Xinyuan, “-Isomeric Cross Section Ratio in the Au-197(n,2n)Au-196 reaction.-”, J, PHE,5, (5),593,1981.

[10] S.K.Mangal, C.S.Khurana,“Isomeric (n,2n) Cross Section at 14.8MeV”,J,NP,69,258,1965.

BAR-MOM Code and Its Application

WANG Shunuan

China Nuclear Data Center, CIAE, P.O.Box 275(41) Beijing 102413

e-mail: wsn@iris.ciae.ac.cn

【**abstract**】*BAR-MOM code for calculating the height of the fission barrier B_f, the energy of the ground state is presented; the compound nucleus stability by limit with respect to fission, i.e., the angular momentum (the spin value) L_{max} at which the fission barrier disappears, the three principal axis moments of inertia at saddle point for a certain nucleus with atomic number Z, atomic mass number and angular momentum L in units of $\hbar$ for 19<Z<102, and the model used are introduced briefly. The generalized BAR-MOM code to include the results for Z≥102 by using more recent parameterization of the Thomas Fermi fission barrier is also introduced briefly. We have learned the models used in Code BAR-MOM, and run it successfully and correctly for a certain nucleus with atomic mass number A, atomic number Z, and angular momentum L on PC by Fortran-90. The testing calculation values to check the implementation of the program show that the results of the present work are in good agreement with the original one.*

In heavy nuclei collision with sufficiently high energies, the composite systems formed may have angular momentum in excess of $100\hbar$. For the system with such large angular momentum, it is important to know whether a locally stable equilibrium configuration of the fused nuclei exists. This is because an equilibrium compound nucleus may not be formed if such a configuration does not exist. After formation of a compound nucleus, the height of the fission barrier strongly affects the probability of fission decay relative to other decay channels. The moments of inertia of the saddle point configuration mainly determine the angular distribution of fission fragments. Therefore, A.J. Sierk[1] presented a macroscopic rotating droplet model of a rotating nuclei with following modifications relative to the liquid drop model: (1) The surface energy of the liquid drop model is replaced by the Yukawa-plus-exponential nuclear energy taking into account of the effects of finite range of the nuclear force, nuclear saturation, and the finite surface thickness of real nuclei[2]. (2) The Coulomb energy is calculated for a certain charge distribution with a realistic surface diffuseness[3]. (3) The rotational moments of inertia are calculated for rigidly rotating nuclei with realistic surface density profiles[3]. (4) The parameters of the model for the various contributions to the energy of the nucleus provide a better fit than do those of the liquid drop model to nuclear ground state masses and fission barriers of non-rotating nuclei [2,4]. (5) A flexible shape parameterization (a new triaxial shape parameterization) is employed, which allows accurate estimation of the convergence of results as a function of the number of the degrees of freedom of the nuclear shapes considered[5]. In addition, highly accurate numerical techniques for the calculation of details of the macroscopic potential energy surface are utilized. From theoretical point of view, nuclear systems with large amounts of angular momentum, which are formed in heavy ion collisions, generally also have high internal excitation energy. For sufficiently high internal excitation energy, shell and pairing effects vanish, and a macroscopic model may be reasonable.

Based on the model described above and using the approximated fit method shown in Ref. [1] and its appendix (BAR-MOM fit), A.J. Sierk developed the code BAR-MOM[6] to calculate the height of the fission barrier B_f, including the energy of the ground state, the compound nucleus stability by limit with respect to fission, i.e., the angular momentum(the spin value) L_{max} at which the fission barrier disappears, the three principal axis moments of inertia at saddle point for a certain nucleus with atomic number Z, atomic mass number and angular momentum L in units of $\hbar$. The calculated results involving many hundreds of nuclei have been approximated in a useable accurate values for L_{max}, B_f (L), and the saddle point three principal axis moments of inertia for any measurable nucleus with $19<Z<102$. The calculated barrier for L=0 are accurate to a little less than 0.1 MeV. The output from BAR-MOM fit is a little less accurate. Worst errors may be as large as 0.5 MeV but the characteristic uncertainty is in the range of 0.1~0.2 MeV. The values of ground state

energy are generally approximated to within about 0.1~0.2 MeV. The approximate value of the stability limit is always within 0.5 $\hbar$ of the calculated one [7]. In the model used in BAR-MOM code, several effects are neglected which may influence the results, for instance, the temperature dependence of the nuclear radius, surface diffuseness constants, and an angular momentum dependence of the diffuseness, the single particle effects and so on.

According to the model introduced and the calculated and fitted results analysis, M. Herman has put the code BAR-MOM together with his well known EMPIRE II statistical model code for nuclear reaction calculations as a part of input parameters library. In addition, he has generalized the BAR-MOM code to include the results for $Z \geqslant 102$ by using more recent parameterization of the Thomas Fermi fission barrier[8] at zero spin, and assumed that angular momentum dependence calculated with BAR-MOM fit for Z=102 and A=256 is also valid for the heavier nuclei. By using the self-consistent Thomas Fermi model backed by liquid drop model scaling rule for fission barriers, Ref. [8] has constructed a simple algebraic equation for Thomas Fermi fission barrier. The equation is accurate for proton numbers greater than about 70 and for neutron number up to at least 20 units on either side of beta stability. This makes it possible to make a comprehensive comparison of the Thomas Fermi theory with 120 measured fission barriers. For nuclei lighter than uranium (fissility $x \leqslant 40$) the calculated values reproduce in rather faithfully the measured trend, with a fairly constant overestimate of about 1 MeV. It should be stressed that the parameters of the Thomas Fermi model were not adjusted in any way to the fission barriers [9]. The overall agreement within 1MeV or so is quite remarkable for fissility $x \geqslant 40$; the measured values decrease more slowly with fissility x than the calculations, building up to an excess over the calculated values of about 1 MeV for fissility $x \geqslant 42$. Generally speaking, the model shows the fission barriers rather well.

In the present work, we have learned the models used in Code BAR-MOM, and run it successfully and correctly for a certain nucleus with atomic mass number A, atomic number Z, and angular momentum L on PC by Fortran-90. Table 1 shows the testing calculation values to check the implementation of the program. It can be seen clearly from the list of table 1 that the calculated results in the present work are in good agreement with that presented in Ref. [7].

The code BAR-MOM is available at CNDC, and it can be used for nuclear data calculation or as an input parameter library for fissional nuclei statistical model calculations. It is also functional in heavy ion physics and other fundamental research of nuclear physics.

Table 1 Testing values to check implementation of the code BAR-MOM

Z	A	L	Egnd st	Fiss Bar	Moments of Inertia			L_{max}
28	58	0	0.00	33.14	0.816	3.603	3.608	46.1*
			0.00	33.15	0.816	3.601	3.601	45.9**
28	58	25	21.36	19.50	0.778	3.662	3.662	45.9*
			21.54	19.51	0.778	3.656	3.656	45.9**
28	58	40	49.66	2.97	0.724	3.648	3.650	45.9*
			50.10	2.90	0.723	3.648	3.654	45.9**
65	153	0	0.00	28.88	0.621	3.698	3.698	82.3*
			0.00	28.88	0.621	3.698	3.698	82.3**
		50	19.00	16.16	0.615	3.639	3.639	82.3*
			19.09	16.16	0.615	3.638	3.642	82.3**
		80	45.24	0.26	0.616	2.765	2.788	82.3*
			45.20	0.27	0.615	2.802	2.802	82.3**
93	229	0	0.00	3.76	0.823	1.747	1.747	68.1*
			0.00	3.70	0.715	1.749	1.749	68.9**
		45	8.21	1.26	0.765	1.578	1.578	68.1*
			8.09	1.24	0.764	1.589	1.589	68.9**

Z atomic number
A atomic mass number
L angular momentum
Egnd st energy of ground state
Fiss Bar Fission barrier
Moments of Inertia three principal axis moments of inertia at saddle point
L_{max} angular momentum (the spin value) at which the fission barrier disappears
* calculated results in Ref[7]
** calculated results in the present work

References

[1] A.J.Sierk, Phys. Rev. C, Vol.33, No.6, 2039(1986)
[2] H.J.Krappe, J.R.Nix, and A.J.Sierk, Phys. Rev.Lett.42, 215(1979); Phys.Rev.C20, 992 (1979)
[3] K.T.R Davies and J.R. Nix, Phys. Rev.C14, 1977 (1976).
[4] P.Möller and J.R.Nix, Nuccl.Phys. A361,117(1981);At. Data Nucl. Data Table 26,165(1981)
[5] S. Tentalange, S.E. Koonin, and A.J. Sierk, Phys. Rev.C22,1159(1980)
[6] BARMOM, #9677, National Energy Software Center, Argonne National Laboratory, Argonne, IL 60439
[7] M.Herman, Workshop on Nuclear Reaction Data and Nuclear Reactors: Physics, Design and Safety, 13 March-14 April 2000, Trieste, Italy, SMR/1220-10
[8] W.D. Myers and W.J. Swiatecki, Phys. Rev. C60, 014606(1999)
[9] W.D. Myers and W.J. Swiatecki, Nucl. Phys. A601, 141 (1996)

Calculations of n+^{112,120}Sn Reactions in the Energy Region up to 20 MeV

DUAN Junfeng[1] HAN Yinlu[2] SUN Xiuquan[1]

1 Department of Physics, Northwest University, 710069

2 China Nuclear Data Center, CIAE

【**abstract**】*A set of optimal neutron optical potential parameter is obtained based on experimental data of total, nonelastic, elastic scattering cross sections and elastic scattering distribution. All cross sections of neutron induced reaction, γ-ray produced cross sections, angular distribution, energy spectrum and double differential cross sections are calculated and analyzed for n+$^{112\ 120}$Sn at incident neutron energies below 20 MeV. All experimental data are taken from EXFOR library and other evaluated data from JENDL-3.*

Introduction

The element stannum (Sn) is one of the important fission product nuclei. ^{112}Sn (abundance is 0.97%) and ^{120}Sn (abundance is 32%) are isotopes of the natural stannum.

In this work, theoretical models are used to calculate and analyze neutron-induced all cross sections and energy spectra below 20 MeV. An overview of the theoretical models used in this work is introduced in Section 1 and the analysis and comparisons of calculated results with experimental data are given in Section 2, a simple conclusion presented in Section 3.

Owing to the absence of experimental data for isotopes ^{112}Sn and ^{120}Sn, the calculated results of total, nonelastic, (n,γ) cross sections, elastic scattering distribution at partly incident energy points, neutron energy spectrum and double differential cross sections are compared with experimental data of natural stannum.

1 Theoretical Models and Parameters

The latest version of the UNF code[1] used on the optical model, the semi-classical model of multi-step nuclear reaction processes, was used to calculate

nuclear reaction cross sections. Direct reactions to low-lying residual nucleus states were pre-calculated by using the distorted wave Born approximation and included as input data for the UNF code.

1.1 Optical Model and Optical Potential Parameters

The optical model was used to calculated total, nonelastic, elastic scattering cross sections and elastic scattering angular distribution, and the transmission coefficient of the compound nucleus. The optical potentials considered here are Woods-Saxon form for the real part, Woods-Saxon and derivative Woods-Saxon form for the imaginary parts corresponding to the volume and surface absorption, respectively, and the Thomas form for the spin-orbit part.

The code APOM[2] was used to automatically adjust the optimal neutron optical potential parameters based on experimental data of total, nonelastic cross sections and elastic scattering angular distributions. The optical potential obtained are as follows:

The real part of optical potential,

V=53.5564–0.37731E_n+0.00353E_n^2–24.0(N-Z)/A

The imaginary part of the surface absorption,

W_s=max{0.0,11.1484–0.1969E_n–12.0(N-Z)/A}

The imaginary part of the volume absorption,

W_v=max{0.0, –2.09778+0.18168E_n–0.00005158E_n^2}

Where E_n is the incident neutron energy and Z, N, A are the number of charge, neutron and mass of the target nucleus respectively.

The spin-orbit couple potential U_{so}=6.2.

The radius of the real part, the surface absorption, the volume absorption and the spin-orbit couple potential

r_r=1.1870, r_s=1.26866, r_v=1.51577, r_{so}=1.1870.

The width of the real part, the surface absorption, the volume absorption and the spin-orbit couple potential

a_r=0.73796, a_s=0.4981, a_v=0.68434, a_{so}=0.73796.

Fig. 1 and Fig. 2 show comparisons of the calculated results of total and nonelastic cross sections for ^{120}Sn with experimental data of natural stannum and they are in good agreement. The calculated results of neutron elastic scattering angular distribution for ^{120}Sn are compared with experimental data of natural stannum at incident energy E_n=5.0, 6.04, 7.0, 8.08 MeV and compared with experimental data of itself at incident energy E_n=0.4, 1.45, 2.57, 3.6, 9.943, 11.0, 13.92, 16.91 MeV. One can see the calculated results are in good agreement with experimental data from Fig. 3(a) and Fig. 3(b). The calculated results of elastic scattering cross sections for ^{120}Sn and total, nonelastic, elastic scattering cross sections and elastic scattering angular distribution for ^{112}Sn are not given due to limitation on space. In the view of the analysis shown above, this set of neutron optical potential parameter is used for n+ ^{112,120}Sn theoretical calculation.

1.2 Direct Inelastic Scattering Cross Sections

The direct inelastic scattering cross sections to low-lying states are important in nuclear data theoretical calculations. The code DWUCK4[3] of the distorted wave Born approximation was used to calculate the direct reaction cross sections and included as input for the UNF code. The direct inelastic scattering cross sections are mainly from contribution of states 1.2569 2^+, 2.1511 2^+, 2.4762 2^+ for ^{112}Sn and mainly from contribution of states 1.1713 2^+, 2.0971 2^+ for ^{120}Sn.

1.3 The Pre-equilibrium and Equilibrium Processes

The semi-classical model of multi-step nuclear reaction processes, in which the discrete level effect in multi-particle emissions as well as the pre-equilibrium phenomenon combining with parity conservation and angular momentum conservation were included, was used to describe the nuclear reaction pre-equilibrium and equilibrium decay processes.

This semi-classical model includes both the the Hauser-Feshbach theory and the exciton model, and the exact Pauli exclusion effect in the exciton state densities was taken into account. The pick-up mechanism was used to describe the composite particle emission processes. Based on the leading particle model, the double differential cross sections for all kinds of particles was obtained. The recoil effect was taken into account in the UNF code in order to keep the energy conservation for whole reaction processes.

all reaction cross sections, angular distributions, double differential cross sections, and neutron energy spectrum were calculated for n+^{112,120}Sn at incident neutron energies below 20 MeV by code UNF with the optical potential parameters shown above, adjusting charged particle optical potential parameters, giant dipole resonance parameters and level density parameters. The equilibrium mechanism dominates reaction process of n+^{112,120}Sn, at the incident energy E_n=14.1 MeV, as an example, the equilibrium processes occupy the percentage of P_{eq}=88.54% and the pre-equilibrium processes only have the percentage of $P_{pre\text{-}eq}$=11.46 for ^{112}Sn, while the equilibrium processes occupy the percentage of P_{eq}=82.8% and the pre-equilibrium processes only

have the percentage of $P_{pre\text{-}eq}$=17.2 for ^{120}Sn.The exciton model parameter K is 500 MeV^3 for ^{112}Sn and 800 MeV^3 for ^{120}Sn in this work. The level density parameters a and pair correction parameters Δ of the Gilber-Cameron level density used in this calculation are given in Table 1.

Table 1 The level density parameters used in this work

Isotope	^{112}Sn		^{120}Sn	
	a	Δ	a	Δ
n,γ	16.265	1.03	15.487	–0.49
n,n'	12.470	1.002	16.501	0.5
n,p	13.757	–0.16	15.973	0.5
n,α	15.313	1.04	18.082	1.2
n,He	16.520	2.61	17.649	2.42
n,d	15.625	1.53	16.678	1.34
n,t	15.426	–0.04	17.327	0.12
n,2n	18.274	–0.95	15.16	–0.31
N,nα	15.545	2.71	17.748	2.51
n,2p	17.315	0.92	16.961	1.58
n,3n	14.507	2.82	10.631	0.1

2 Theoretical Results and Analysis

The comparisons between calculated results of (n,γ) reaction cross sections with experimental data of natural stannum are given in Fig. 4. One can see that the (n,γ) cross sections for different isotopes become smaller as the isotope mass A increases. The calculated results of the inelastic cross sections are not given due to the absence of the experimental data, but the calculated results are reasonable based on the discussion on the calculated results of double differential cross sections. The comparison of calculated results of ^{120}Sn (n,2n) cross sections with experimental data is shown in Fig. 5. Fig. 6 shows the comparisons between calculated results of ^{112}Sn (n,p) cross sections with experimental data and JENDL-3. The comparisons of (n,α) cross sections for ^{120}Sn with experimental data of itself are given in Fig.7. The calculated results are in good agreement with experimental data taken from Ref. [8] in energy region 13.3~15.0 MeV, while for E_n>15.0 MeV, it seems that the present results are more reasonable.

The present calculated results of cross sections for all reaction channels are similar to the evaluated results of JENDL-3 in curve shapes, but fit experimental data better than JENDL-3.

In this work, the energy spectrum and double differential cross section were calculated based on the reasonableness of calculated results for all reaction cross sections.

The calculated results of double differential cross sections are compared with experimental data of natural stannum taken from Ref. [9]. The comparisons between the calculated results of ^{112}Sn with the experimental data of the incident energy E_n=14.1 MeV at θ=15°, 40°, 70°, 100°, 130°, 160° are given in Fig. 8. In Fig. 9, the comparisons between the calculated results of ^{120}Sn with the experimental data of the incident energy E_n=14.1 MeV at θ=15°, 40°, 70°, 100°, 130°, 160° are given. The calculated results fit the experimental data in emission neutron energy region 5.0~11.0 MeV, which comes mainly from contribution of inelastic reaction. It shows calculated results of inelastic cross sections are reasonable at incident energy E_n=14.1 MeV.

The calculated results of energy spectrum for ^{112}Sn and ^{120}Sn at incident energy E_n=14.1 MeV are compared with experimental data of natural stannum taken from Ref. [9] and Ref. [10] at incident energy E_n=14.1 MeV and E_n=14.63 MeV in Fig. 10. From Fig. 9 and Fig. 10, one can see that calculated energy spectrum and double differential cross sections for ^{120}Sn are lower than experimental data in emission neutron energy region 0~2.0 MeV which comes mainly from (n,2n) reaction.

3 Summary

In this work, all cross sections of neutron induced reaction, angular distribution, energy spectrum and double differential cross section are calculated. Since the recoil effect is taken into account, the energy for whole reaction processes is balance. A set of optimal neutron optical potential parameter was obtained by code APOM for n+^{112,120}Sn reaction, and theoretical results are in agreement with experimental data. Therefore, this work also demonstrates the reasonability and dependability of these theoretical calculation programs APOM, DWUCK and UNF.

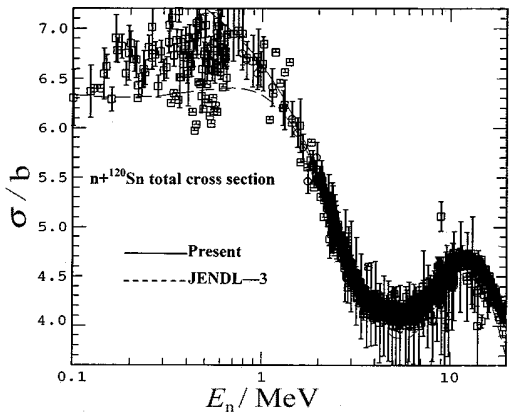

Fig. 1 Comparisons of neutron total cross sections between the calculated values and the experimental data for ^{120}Sn

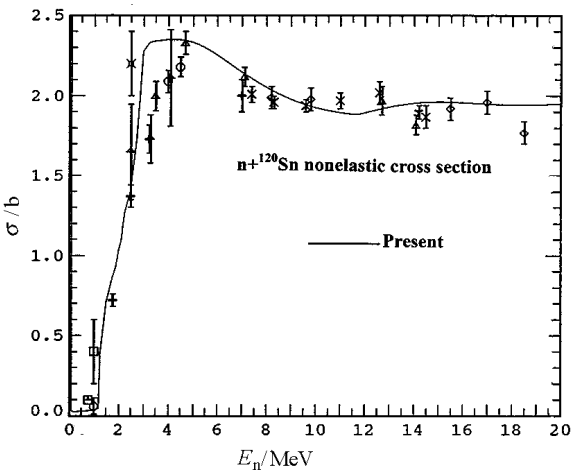

Fig. 2 Comparisons of neutron nonelastic cross sections between the calculated values and the experimental data for ^{120}Sn

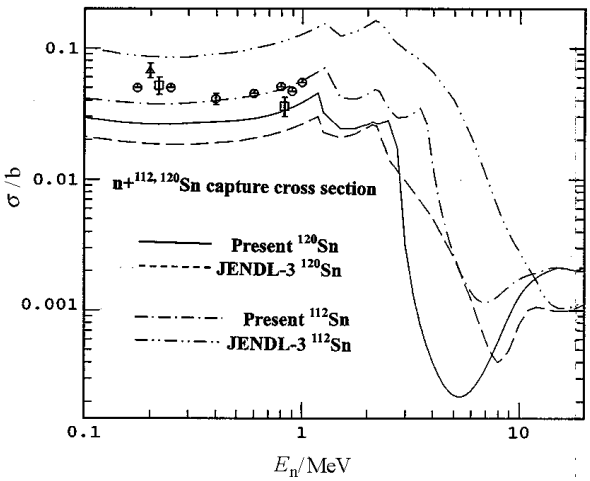

Fig. 4 Comparisons of (n,γ) cross sections between the calculated values and the experimental data

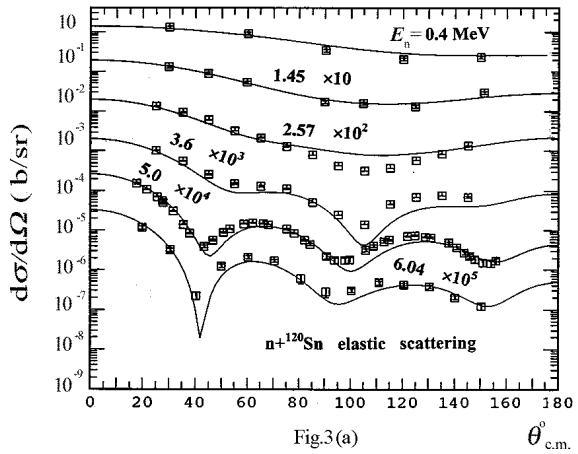

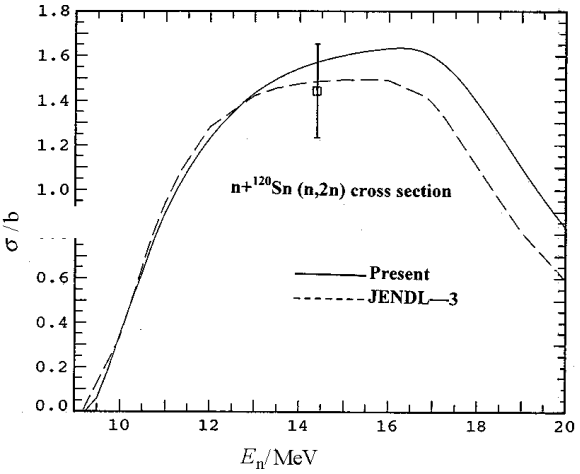

Fig. 5 Comparisons of (n,2n) cross sections between the calculated values and the experimental data for ^{120}Sn

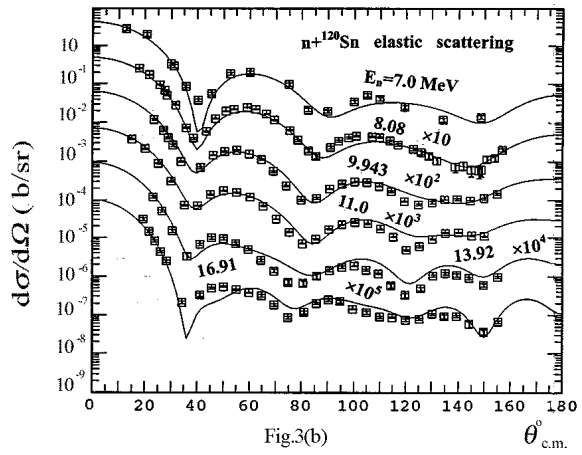

Fig. 3 Comparisons of neutron elastic scattering angular distribution between the calculated values and the experimental data for ^{120}Sn

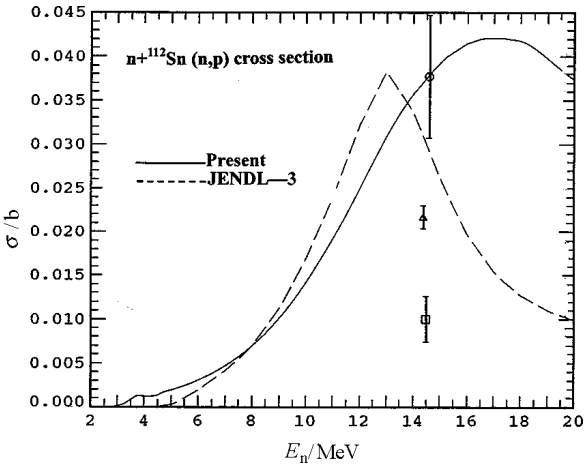

Fig. 6 Comparisons of (n,p) cross sections between the calculated values and the experimental data for ^{112}Sn

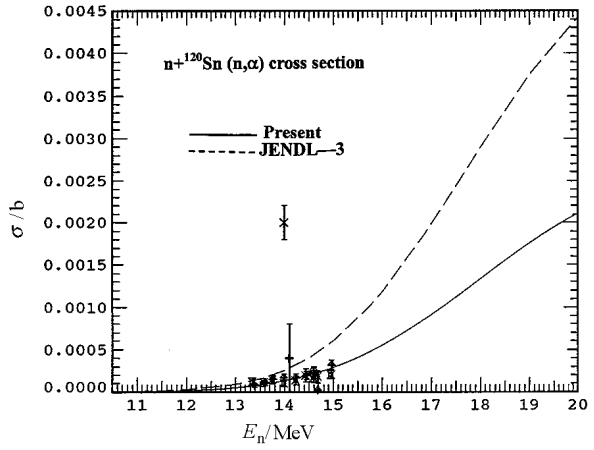

Fig. 7 Comparisons of (n,α) cross sections between the calculated values and the experimental data for ^{120}Sn

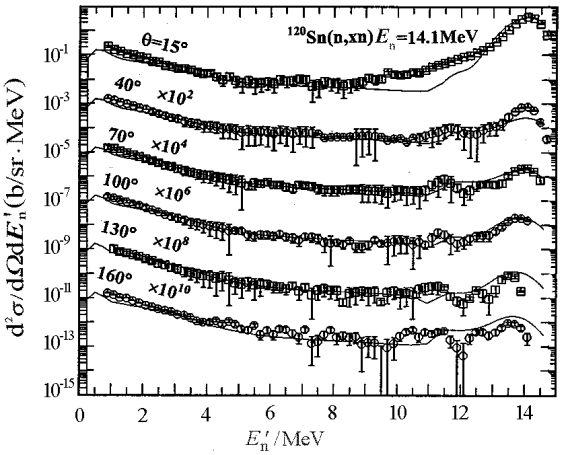

Fig. 9 The same as Fig.8 but for ^{120}Sn

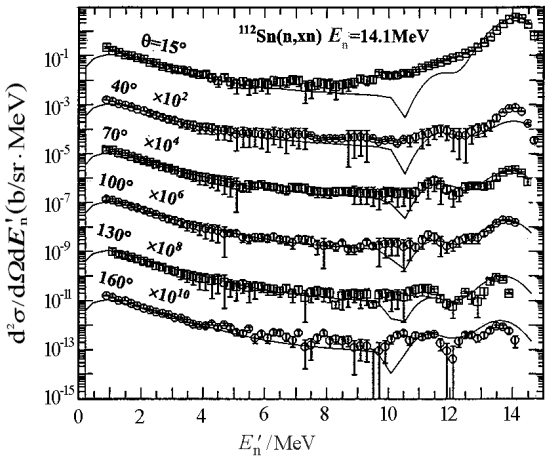

Fig. 8 Comparisons of double differential cross sections between the calculated values and the experimental data for ^{112}Sn

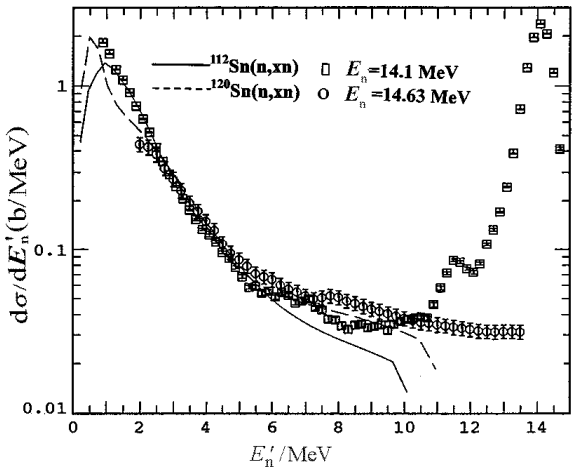

Fig. 10 Comparisons of neutron energy spectrum between the calculated values and the experimental data

References

[1] ZHANG Jingshang, Comm. Nucl. Data Prog. 23,18(2000)

[2] SHENG Qingbiao, Commun. Nucl. Data Prog, 7,43(1992).

[3] P.D.Kunz, DWUCK4 Code.

[4] B.C.Diven, et al. Phys. Rev. 120, 556, 6010.

[5] S.Lulic, et al. J. NP/A, 119, 517, 6811.

[6] P.M.Gopych, et al. C, 87KIEV, 3, 295, 8709.

[7] G.P.Chursin, et al. J, ZET, 44, 472, 6302.

[8] Y.Ikeda, et al. R, JAERI—1312,88.

[9] Takahashi, et al. R.JAERI-M-90-220, 9012.

[10] D.Hermsdorf, et al. J, KE, 19, 241, 7608.

Evaluation of Prompt and Delayed Neutron Yields for ^{239}Pu from 10^{-5} eV to 20 MeV

YU Baosheng CHEN Guochang

China Nuclear data Center, CIAE, P.O.Box275(41), Beijing 102413

e-mail : bsyu@iris.ciae.ac.cn

【**abstract**】*The number of prompt (ν_p) and delayed (ν_d) neutrons emitted per fission event was evaluated for ^{239}Pu based on absolute measurements and relative to the spontaneous fission ν of ^{252}Cf. The dependence of prompt neutron number on incident neutron energy for ^{239}Pu was given from 10^{-5} eV to 20 MeV.*

Introduction

The accurate number of prompt and delayed neutron in neutron-induced fission of ^{239}Pu is required along with the quick development for fast reactors and nuclear system concerned. Due to the mean neutron energy of fast reactors is in a few hundred keV regions, the accurate data are very important. For nuclear technique application, the number of neutron emitted per fission event is required with the accuracy from 0.25% to 0.5% in general. The data were evaluated based on the experimental data available and compared with ENDF/B-6 and JENDL-3.

1 Evaluation of Prompt Neutron Yield

The experimental data of prompt and delayed neutron yields were measured by using absolute and ratio measurement techniques. The main measured data[1~17] from 1956 up to now were collected, analyzed and evaluated and they are all summarized in Table 1.

In order to measure absolutely the prompt fission neutron yields, the fission number induced by neutron and the prompt neutron should be detected simultaneously. The fission fragments could be detected by using a high-speed methane-filled ionization chamber. The high efficiency neutron detector is required for detecting prompt neutron. It can be detected by using two different techniques. First, the large liquid scintillator stank was adopted in generally. But this kind detector is also sensitive for γ-ray, so the measured data have large γ-ray background. Second, the proportional counter system was used, which consists of 24 ^{3}He counters in cylindrical paraffin block (or using Born counters with organic moderator). The detector was calibrated with serial neutron sources. The γ-ray background was reduced for this kind of detector.

The ν_p was also measured relatively to spontaneous fission ν_p of ^{252}Cf. The difference of detector efficiencies for fragment and neutron from ^{252}Cf and ^{239}Pu fission was taken into account. Many important corrections were performed along with the development of the nuclear technique. The accurate data have been carried out mainly since 1970.

The early data were measured by J. C. Hopkins[1] from 0.25 MeV to 14.5 MeV, H. Conde[3] from 4.22 MeV to 14.8 MeV and M. Soleihac[4] from 0.36 MeV to 14.78 MeV, respectively. The data published by J. Frehaut[16] revised results of M. Soleihac from 1.36 MeV to 14.79 in 1980. The data of J. Frehaut[16] were measured by using large gadolinium-liquid scintillator tank and made corrections in detail for background neutron, dead time losses, spurious fission, variation of the neutron detector efficiency with the fission counts and the change in the counter efficiency with the background rate. The data were adopted.

Table 1 Information concerning prompt neutron yields for ^{239}Pu(n,f) reaction

Year	Author	En , MeV	Detector	Monitor	Monitor ν	Comment
1980	J. Frehaut	22.79~28.28	SCIN	^{235}U(n,f)	3.782	T-O-F
1980	J. Frehaut	1.36~14.79	SCIN	^{235}U(n,f)	3.732	Modified data of M.Soleihac
1980	Zhang Huanqiao	0.186~1.44	STANK	H(n,n)		
1976	J. A. Khokhlov	1.06~1.81	SCIN	^{252}Cf(0,f)		With large
1975	B. Nurpeisov	0.7~4.89	PROPC	^{252}Cf(0,f)	3.756	
1973	K. E. Volodin	0.08~0.7	PROPC	^{239}Pu(n,f)	3.756	
1973	K. E. Volodin	2.53E-8~1.6	PROPC	^{252}Cf(0,f)	3.756	
1973	J. Frehaut	7.8E-6~4.7E-4	STANK	^{252}Cf(0,f)	3.78	Measured Resonance
1973	J. W. Boldeman	0.2~1.9	STANK	^{252}Cf(0,f)	3.782	COINC.,3MV VDG
1970	M. B. Savin	0.89~4.7	STANK	^{252}Cf(0,f)	3.772	
1970	V. G. Nesterov	0.4~1.6	PROPC FISCH	^{252}Cf(0,f)	3.782	VDG
1970	M. Soleilhac	0.21~1.375	STANK	^{252}Cf(0,f)	3.782	T-O-F
1969	M. Soleilhac	0.36~14.78	STANK	^{252}Cf(0,f)	3.782	T-O-F
1968	H. Conde	4.22~14.8	STANK	^{252}Cf(0,f)	3.764	T-O-F 5 MV,VDG
1965	D. S. Mather	0.99~4.02	STANK	^{252}Cf(n,f)	3.782	6 MV,VDG
1963	J. C. Hopkins	0.25~14.5	STANK	^{252}Cf(0,f)	3.771	
1960	J. Leroy	14.2	BF3	^{238}U(n,f)	4.55	CCW
1958	G. N. Smirenkin	4.0~15.0	FISCH	^{239}Pu(n,f)	2.9	
1956	I. Johnstone	14.1	PROPC FISCH	^{235}U(n,f)		CCW

STANK: Large Liquid Scintillation Detector
SCIN: Gadolinium-Loaded Liquid scintillation Tank
FISCH: Fission Chamber for Fragments Detector
PROPC: BF3 Proportional Counter
COINC: Fission Fragments Detected in Coincidence with Prompt Fission Neutrons.

Around 14 MeV, there are data measured by J. C. Hopkins, M. Soleihac and J.Frehaut[17]. The data measured by J.C.Hopkins with large background and systematic diverge were abandoned. The data measured by J. Ferehaut[16,17], M.Soleihac consist with each other within errors and were renormalized to recommended standards.

In order to obtain the energy dependence of prompt neutron data up to 20 MeV, the data from 22 MeV to 28 MeV measured by J. Ferehaut were used. They were renormalized to recommended standards. In this case, the experimental data were available from 1.63 MeV to 14.9 MeV [16] and 22 MeV to 28 MeV.

For 0.1 to 5 MeV, the data were measured by D.S.Mather[5], M.Soleilhac[6], V.G.Nesterov[7], M.B.Savin[8], J.W.Boldeman[9], K.E.Volodin[11,12], B.Nurpeisov[13], J.A.Khokhlov[14], ZHANGH uangqiao[15] and J.Frehaut. The data measured by V.G.Nesterov, K.E.Volodin, B.Nurpeisov and J.A.Khokhlov were from the same group. The data by B.Nurpeisov were measured by using proportional ^{3}He counters as neutron detector, which consists of 24 ^{3}He counters in cylindrical paraffin block. The neutron detector system was calibrated by serial neutron sources. The γ-ray background was reduced. The multiplayer ionization chamber with 85% counting efficiency was used for detecting fission fragment. The difference of detector efficiencies for fragments and neutrons of ^{252}Cf and ^{239}Pu fission was taken into account. The corrections were made for pulse pile-up from one fission event, energy dependence of detector efficiency, slow neutron influence and pulse-height discrimination from fission fragment. The data by K.E.Volodin and B.Nurpeisov were adopted.

The data by J.W.Boldeman were measured with a 240 L gadolinium-loaded liquid scintilator and a high-speed methane-filled double ionization chamber in energy region from 0.2 MeV to 1.9 MeV in 1973. The coincidences technique between fission fragment and prompt neutron was used to avoid alpha pile up. The time-of-flight method was used to improve the ratio of induced fission to spontaneous fission. The corrections concerned were carried out. The data are quite accurate.

The data by D.S.Mather only provided in several energy bins between 0.99 MeV and 4.02 MeV. The data were measured by J.A.khokhlov by using Born counters with organic moderator at linear electron accelerator. The corrections were made for dead–time, uncertainty of isotope content and fission-spectrum difference of measured ^{239}Pu and monitor nucleus ^{252}Cf. The data were given only at 1.06 MeV and 1.8 MeV with large statistical errors. So the data were abandoned.

The data were measured by ZHANG Huanqiao by using Li(p,n) and T(p,n) monoenergetic neutron sources from 0.7 MeV to 1.8 MeV. A gadolinium-load liquid scintillator in spherical aluminum container was used. The neutron detector efficiencies were measured with H(n,n) reaction. The corrections were carried out for background effects, dead-time loses, delayed γ-ray effects and so called "France effect" (the detecting efficiency for the prompt fission γ-ray has a bearing on the fission neutron number in liquid scintillator tank). The data consist with B.Nurpeisov, J.B.Boldeman[9] within errors.

The data measured by J.B.Boldeman, K.E.Volodin, B.Nurpeisov, ZHANG Huanqiao and J.Frehaut are consistent with each other within errors.

Below 0.1 MeV, there were two sets of data measured by J.Frehaut from 0.78 keV to 0.47 keV and K.E.Volodin at 0.0253 eV and 0.08 eV. The tend of the data was mainly determined by J.Frehaut. It is shown that some minor structures were observed in the energy dependence of ν_p .

The data measured by K.E.Volodin[11] and E.Barnard[18] at thermal energy point consist with the data evaluated by N.E.Holden[19]. The measured data were adopted.

2 Recommendation of Prompt Neutron Data

2.1 The Reference Standard of ^{252}Cf

The ν_p-value for the spontaneous fission of ^{252}Cf is usually used as the reference standard. The distinct advantages of ^{252}Cf are its relatively high spontaneous fission rate with respect to its alpha decay rate and the high intensity spontaneous fission neutron source could be produced easyly.

Before 1972, the prompt neutron number derived from large liquid scintillator is 7% systematically higher than the one derived by $MnSo_4$ bath experiments, and the errors of themselves of those measured data were larger than 1 %. Through the improvement of measured method, it was found that this comes from the effects of delayed γ-ray and called "France effect". In 1972, at IAEA Panel on Neutron Standard Reference Data[20], a preliminary value 3.724±0.008 was recommended based on experimental data and taken into the systematical high value for liquid scintillator measurement.

In addition, the corrections are required in ν_p measurements for differences of the efficiencies of neutron detector for the fission neutron spectrum. Therefore, the improvement of neutron detection and reasonable corrections were specially paid attention in the evaluation at that time. The ν_p value for the reference standard ^{252}Cf was discussed and reevaluated in IAEA Consultant's meeting in 1988. The recommended value ν_p was 3.7661±0.054 [21]. The accuracy of the value for this standard is adequate for all current applications of ν_p value.

2.2 Recommendation of the Data

The accurately measured data[11~13,15~19] were adopted in this work. The most of measured data were performed relatively to ^{252}Cf spontaneous fission as standard, taken as 3.7661±0.054. The relatively measured data were renormalized. The absolutely measured data by ZHANG Huanqiao were very accuracy. A weighted least squares fitting was applied to get the dependence on incident neutron energy from 10^{-5} eV to 20 MeV. The evaluated dates shown in Fig. 1 were compared with ENDF/B-6 and JENDL-3.2.

3 Evaluation and Adjusting of Delayed Neutron Yields

Accurate delayed neutron yield data are vital to the development of fast reactor static and demonic calculations and to the modification fission physics researches.

The delayed neutron yield data were measured by G.R.Keepin[22] , C.F.masters [23] and M.S.Krick [24], respectively. M.S.Krick studied the dependence of delayed neutron yield on the induced fission neutron energy in detail. It was found that the delayed neutron yield is independent of the neutron energy from 0.1 to 4 or 5 MeV, then drops in an energy interval of ~2 MeV to the energy measured 14.9 MeV.

In order to recommend the accurate delayed neutron yield data, the data measured were considered and revised by A.E.Evans[25]. Some identical fission foils were used in fission chambers to monitor fission rates in the samples. And also a single ^{238}Pu-Li neutron source was used to calibrate delayed neutron detectors, which was certified by the National Bureau of Standards of USA. The calibration result for ^{238}Pu-Li neutron source

indicated that the yield measured by C.F.masters and M.S.Krick are 4.6 % higher and should be reduced accordingly. Furthermore, the quantity of fission foils used in sample was remeasured by using a low geometry alpha-country system with-well determined accuracy. The remeasured value was in agreement within 1% with the value of the foils used, so the yield values were not adjusted for the sample.

On the basis of these considerations mentioned above, the delayed neutron data measured by C.F.masters and M.S.Krick were corrected for calibration source, and the new revised values were adopted in this work. The evaluated delayed fission neutron yields are shown in Fig. 2 compared with ENDF/B-6 and JENDL-3.2.

The total fission neutron yields are the sum of prompt and delayed fission neutron yields, shown in Fig. 3 with the data from ENDF/B-6, JENDL-3.2 and calculated.

4 Discussion

The evaluations[26,27] for number of neutrons emitted per fission were carried out below 15 MeV based on experimental data. In present work, there are new measured data and the energy region was extended. The data measured absolutely by Zhang Huanqiao from China Institute of Atomic Energy from 0.2 MeV to 1.44 MeV in 1988 consist with the relative measurement method within errors. So the evaluated data are more reliable due to based on both of absolute and relative measurements. In present work, recommended delayed neutron yields for ^{239}Pu are in good agreement with the measured data available. The dependences of prompt and delayed emission number on incident neutron energy were given from 10^{-5} eV to 20 MeV.

In the case of prompt neutron, it seems that there exist some fluctuations associated with the resonance in the low-energy range as shown in Fig. 4. But the magnitudes of such structures are somewhat different and need to be determined further. It was demonstrated that these fluctuations could make a significant impact on the reactor k_{eff}. The structures were given in ENDF/B-6 based on the data measured by J.Frehaut[10], but they were not given in this work and JENDL-3. In order to investigate these constructures, further measurements are required, which should be with much smaller energy dispersion for the incident neutron and with a special emphasis on the fluctuations.

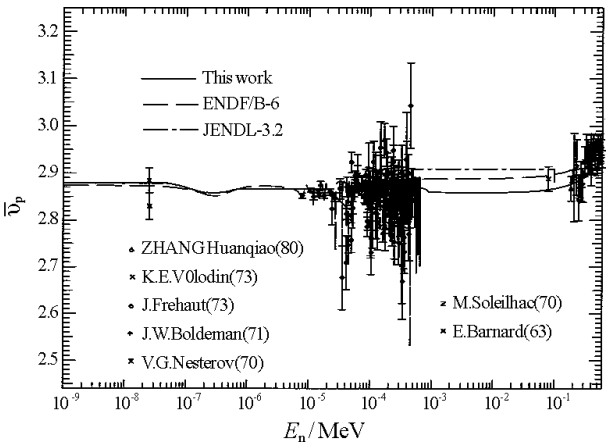

(a)

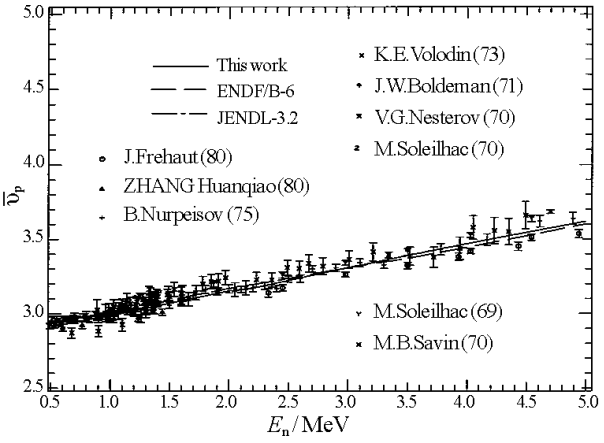

(b)

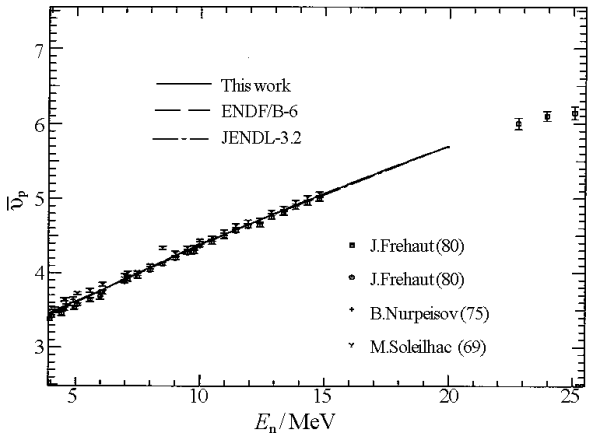

(c)

Fig. 1 Comparison of evaluated and measured prompt neutron yield for ^{239}Pu

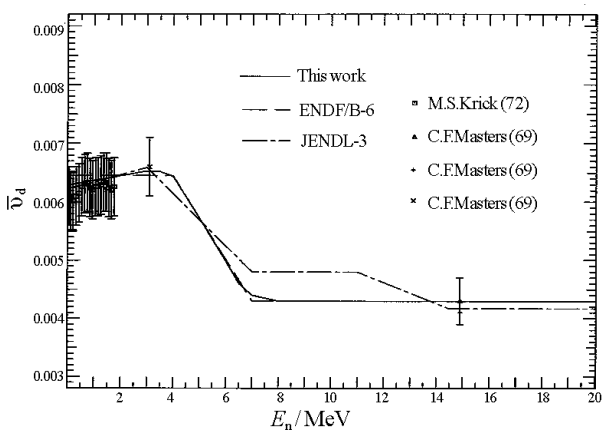

Fig. 2 Comparison of evaluated and measured delayed neutron yield for ^{239}Pu

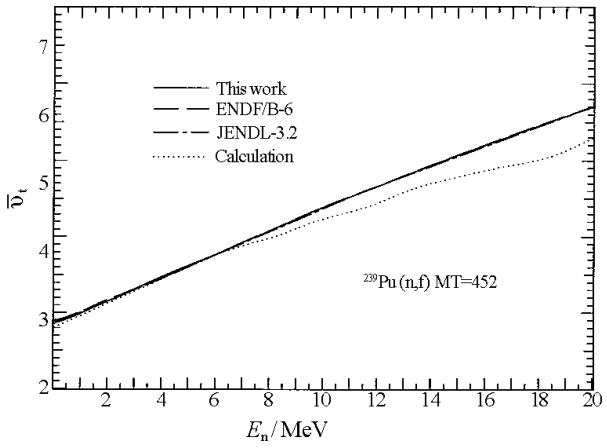

Fig. 3 Comparison of evaluated total fission neutron yield for ^{239}Pu

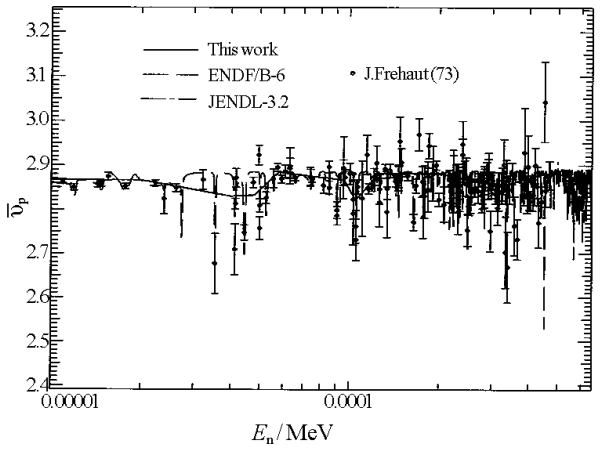

Fig. 4 Comparison of evaluated and measured prompt neutron yield for ^{239}Pu

Acknowledgments

The authors are indebted to CNNC (China National Nuclear Corporation) and CIAE for their supports and would like to extend their thanks to Professors ZHANG Huanqiao, Han Hongyin, TANG Guoyou and SHI Zhaomin for the interesting and useful discussions.

References

[1] J.C.Hopkins et al. Nucl. Phy., 48,433(1963)
[2] D.S.Mather et al. Nucl. Phy.,66,149(1965)
[3] H.Conde et al. J.JNE,22,53(1968)
[4] M.Soleilhac et al. Nuclear Energy,23,257(1969)
[5] D.S.Mather et al. AWRE-0-42/70(1970)
[6] M.Soleilhac et al. Conf. on Nuclear Data for Reactors, Helsonki, Finlad, Vol. 2,145(1970)
[7] V.G.Nesterov et al. EXFOR Data N0.40033003
[8] M.B.Savin et al. Conf. on Nuclear Data for Reactors, Helsonki, Finlad, Vol.2,157(1970)
[9] J.W.Boldeman et al. Ann. Nucl.Sci.Eng.,1,353(1974)
[10] J.Frehaut et al. Symp. on Physcs and Chemistry of Fission, Rochester, USA,Vol.2,20(1973)
[11] K.E.Volodin et al. AE 33,901 (1973)
[12] K.E.Volodin et al. ibid.
[13] B.Nurpeisov et al. AE,39.199(1975)
[14] J.A.Khokhlov et al. EXFOR Data 40523002(1976)
[15] ZHANG Huaqiao et al. J. China Nuclear Physics,2,29(1980)
[16] J.Frehaut et al. EXFOR Data 20490003(1980)
[17] J.Frehaut et al. EXFOR Data 21685004(1980)
[18] E.Barnard et al. Nucl. Phy.,71,228(1965)
[19] N.E.Holden et al. Nucl.Sci.Eng., 98,174(1988)
[20] E.J.Axton et al. IAEA-PL-2646-2/31(1972)
[21] J.W.Boldeman et al. INDC(NDS)-220, 21(1989)
[22] G.R.Keepin et al. Phys.Rev.,107,1044(1957)
[23] C.F.Masters et al. Nucl.Sci.Eng., 36,202(1969)
[24] M.S.Krick et al. Nucl.Sci.Eng., 47,311(1972)
[25] A.E.Evans et al. Nucl.Sci.Eng., 50,80(1973)
[26] F.Manera et al. J. REA,10,637(1972)
[27] LIU Zuhao et al. Hsj-75007(1976)

The Cross Section Evaluation and Recommendation of ^{197}Au (n,2n)^{196}Au Reaction

FAN Sheng YU Baosheng LIU Tingjing

China Nuclear Data Center, CIAE, P.O.Box 275(41) Beijing 102413

e-mail: sfan@iris.ciae.ac.cn

【**abstract**】*The evaluation for ^{197}Au(n,2n)^{196}Au cross section was performed, the data of this reaction in the neutron energy range from threshold to 30 MeV were given, compared with the evaluation results by YUAN Hanrong et al., ZHAO Wenrong et al., Jose Martinez-Rico and YU Baosheng et al.. The agreement between different evaluations is good. However, the deviations are shown up for the data from ENDF/B-6 and JEF-2.2.*

Introduction

The ^{197}Au(n,2n)^{196}Au is one of the important dosimetry reaction. More than 40 measurements have been reported. Most of the experimental data were carried out by using the activation method and a few of them were carried out by using the large liquid scintillators.

The recent evaluations were reported by Yuan Hanrong[1] et al., ZHAO Wenrong[2] et al., Jose Martinez-Rico[3] and YU Baosheng[4] et al. The comparison among them are shown in Fig. 1. The agreement among the differential evaluations is good. However, the deviations are shown up in the energy region from 12 MeV to 20 MeV. The evaluation of Jose Martinez-Rico is not smooth from the threshold to 20 MeV, the data are lower in the range from 13 MeV to 15 MeV. The results of the evaluation are also compared with the ENDF/B-6 and JEF-2.2. The neutron energy extends to 30 MeV for ENDF/B-6, and the data are lower at the energy lower than 14 MeV, and higher in the energy range from 14 MeV to 20 MeV. For JEF-2.2, the data is larger in the energy range from 13 MeV to 16 MeV, and lower in the energy larger than 16 MeV.

The values of the different evaluations at the energy 14.7 MeV, YUAN Hanrong et al. is 2094±40 mb, ZHAO Wenrong et al., 2137±40mb, Jose Martinez-Rico, 2126±26mb, YU Baosheng et al. 2133±34 mb and T.B.Ryves[5] et al., 2127±26 mb, ENDF/B-6, 2187 mb. All evaluations were performed based on the experimental data before 1989.

In present work, we collected the new experimental data and re-evaluate the cross section of ^{197}Au(n, 2n)^{196}Au at the energy 14.7 MeV. And the cross section in the neutron energy range from threshold to 30 MeV was recommended.

1 The Evaluation of the Data at the Energy 14.7 MeV

In Table 1 are shown the measurements[6~35] for the cross section of ^{197}Au(n, 2n)^{196}Au at 14.7 MeV and their adjusted values. The R_1 is an adjusted factor for neutron energy according to the evaluation curve of T. B. Ryves[5], and R_2 is an adjusted factor for standard cross section and gamma branching, the standard cross section of ^{27}Al(n,α) reaction are taken from ENDF/B-6.

From Table 1, it can be seen that most of the data were measured relatively. The threshold energy of ^{197}Au(n,2n)^{196}Au reaction is 8.112 MeV, and the threshold energies of used as standard reactions ^{27}Al(n,α) is 3.248 MeV; ^{93}Nb(n,2n), 8.926 MeV; ^{75}As(n, 2n), 10.382 MeV; ^{56}Fe(n,p), 2.965 MeV; and

Table 1 ^{197}Au(n, 2n)^{196}Au experimental data

No.	Year	Author	E_n/MeV	σ_0/mb	$\Delta\sigma$/mb	Monitor	σ_0/mb (for Monitor)	R_1	R_2	σ/mb	Neutron source	METHOD	Detector	error	note
1	1969	R.C.BARRALL	14.6±0.2	2070	200	^{27}Al(n, α)		1.001		2072.	(D-T) T(d,n)	Activation	NaI(Tl)	200	√
2	1972	A.K.HANKLA	14.4±0.4	1986.	150.	^{27}Al(n, α)	151±18	1.003	0.7815	1556.	(D-T) T(D,N)	Activation	GE(LI)		×
3	1972	D.R.NETHAWAY	14.72	2149.		^{27}Al(n, α)	117.0±0.8	0.997	0.9658	2069.	(D-T)			200	√
4	1977	L.R.VEESER	14.7±0.15	2064.	125.0	H(n,n)H		1.000		2062.	(D-T)	Capture gam-rays detected	Liquid Scintillator		×
5	1975	B.P.BAYHURST	14.10±0.05 14.89±0.05	2213. 2116.	94. 89.	^{27}Al(n, α)	122.0 107.0	1.006 0.9981	0.9959 1.0374	2217 2190	(D-T)	Activation	NAI(TL)	221 89	√ √
6	1960	H.A.TEWES	14.5	2080.		H(n,n)H		1.001		2082	(D-D)	Activation	Recoilo proton counter telescope		×
7	1961	R.J.PRESTWOOD	14.81	2356.	118.	^{238}U(n,f)	145.1±7.3	0.9990		2354	(D-T) T(D,N)	Activation			×
8	1987	L.R.GREENWOOD	14.50 14.65 14.80	2151. 2154. 2171.	33. 33. 33.	^{93}Nb(n,2n)	463±18	1.001 1.0004 0.9990	0.9905 0.9905 0.9905	2132 2134 2128		Activation	GELI	33 33 33	√ √ √
9	1975	J.FREHAUT	14.76±0.065	1935.	155.	^{238}U(n,f)	1216	0.9994		1934	(D-D)		Liquid Scintillator		×
10	1975	A.PAULSEN	14.4 ±0.44 14.6 ±0.32 14.8 ±0.34	1870. 1880 1890	105. 105. 105.	H(n,n)H		1.003 1.001 0.9990		1876 1881 1888	c T(D,N)		GELI		× × ×
11	1972	S.M.QAIM	14.7±0.3	2209.	253.	^{75}As(n,2n)	970±80	1.000		2209	(D-T)	Activation	GELI	253	√
12	1972	D.S.MATHER	14.3	2578.	177.	^{238}U(n,f)	1169±230	1.004		2588	(D-T)		Scintillator		×
13	1968	W.DILG	14.7±0.15	2320	150.	^{27}Al(n, α)	111.5±1.7	1.000	1.018	2361	(D-T)	Activation	NAI(TL)		×
14	1978	P.ANDERSSON	14.9±0.2	2295	116	H(n,n)H		0.9980		2290	(D-T)	Activation	GELI		×

Cont. Table 1

No.	Year	Author	E_n/MeV	σ_0/mb	$\Delta\sigma$/mb	Monitor	σ_0/mb (for Monitor)	R_1	R_2	σ/mb	Neutron source	METHOD	Detector	error	note
15	1981	J.LAUREC	14.8±0.3	2010.	90.	^{27}Al(n, α)	112.0±0.2	0.9990	1.0089	2026	(D-T)	Activation	GELI	202	√
16	1981	T.B.RYVES	14.68±0.03	2170	67.	^{56}Fe(n,p)		1.0002	0.9940	2144	(D-T)	Activation	GELI	67	√
17	1984	Y.IKEDA	14.66	2120.	106.	^{27}Al(n, α)		1.0004		2121	(D-T)	Activation	GE-IN	106	√
18	1988	Y.IKEDA	14.71	1894.	97.	^{27}Al(n, α)	129.1±7.0	1.0000	0.8760	1659	(D-T)	Activation	GELI		×
20	1988	K.KOBAYASHI	14.05±0.07	2125.	79.	^{27}Al(n, α)	123±3.8	1.0060	1.0000	2137	(D-T)	Activation	GELI	79	√
21	1990	I.KIMURA	14.1	2125.	79.	^{27}Al(n, α)	123±3.8	1.0060	0.9878	2111		Activation		200	√
22	1972	D.MAOR	14.0	2200.	300.			1.007		2215		Activation	GELI	200	√
23	1989	LU HAN-LIN	14.6	2129.	95.	^{27}Al(n, α)	115.8±1.6	1.000	1.0000	2129	(D-T)	Activation	GELI	95	√
24	1982	J.CSIKAI	14.66	2087.	142.	^{27}Al(n, α)	122 (14.1)	1.0004	1.0000	2088	(D-T)	Activation	GELI	142	√
25	1982	A.REGGOUG	14.8	1990	50			0.9990		1988	(D-T)	Activation	GELI		×
26	1984	M.HERMAN	15±0.3	2025. 2148.	122. 137.	^{56}Fe(n,p)		0.9980		2021 2143	(D-T)	Activation	GELI	 137	× √
27	1984	I.GARLEA	14.75	2071.	93.	^{238}U(n,f)	2021	0.9994		2070	(D-T)	Activation	GELI	200	√
28	1989	WANG XIUYUAN	14.67±0.24	2147.	114.	^{27}Al(n, α)	115.3±2.7	1.0003	1.0035	2155		Activation		114	√
29	1989	WANG XIUYUAN	14.63±0.15	2133	155	^{27}Al(n, α)	115.3±2.7	1.0006	1.0035	2142		Activation		155	√
30	1965	S.K. MANGAL	14.8	1720.	172.	^{27}Al(n,p)	230±35	0.9990		1712			Scintillator		×
31	1992	I.GARLEA	14.758±0.3	1896.	85.	^{93}Nb(n,2n)		0.9995		1895	(D-T)	Activation	GELI		×
32	1972	G.N.MASLOV	14.2±0.2	2243.	160.	^{65}Cu(n,2n)	920±20	1.0050	0.9964	2237		Activation	Scintillator	160	√
33	1972	D.R.NETHAWAY	14.43	2168	100.	^{27}Al(n,p)		1.0024	1.0074	2189				100	√
33	1997	A.A.FILATENKOV	14.67	2325.	120.	^{27}Al(n, α) ^{93}Nb(n,2n)	128.9±5.6	1.0004	0.9535	2225		Activation	Scintillator	222	√
34	1999	A.A.FILATENKOV	14.1	2220.	90.	^{27}Al(n, α) ^{93}Nb(n,2n)	128.9±5.6	1.0060	0.9535	2129		Activation	Scintillator	90	√
35	1989	T.B.RYVES	14.7	2127.	26.			1.0000		2127				26	√

^{65}Cu(n,2n), 11.399 MeV. For H(n,n)H reaction, the threshold energy is zero. The threshold energy of the standard reaction ^{93}Nb(n,2n) is closed to the reaction ^{197}Au(n, 2n)^{196}Au, the data using this standard should be in agreement with the true values of the reaction ^{197}Au(n,2n)^{196}Au. In contrary to the standard reaction H(n,n)H, the results maybe have large error, because the low energy neutron effect. We divide the data at around 14 MeV into four groups: relative measurements to reaction ^{27}Al(n,α), H(n,n)H, ^{238}U(n,f) and others. The result is shown in Fig. 2. It was found that the results with H(n,n)H reaction are much lower than other three groups, the systematic errors should be existed in these measurements, so the data were given up. Some of the data in other three group are abnegated since they are far away comparing with other experimental data. In Table 1, the data with "√" denotes the experimental data being adopted, and "×" denotes the data being given up.

The errors acting as weight were adjusted. In Table 1, if there are no errors given by the author, or the errors are lower than 5%~15% for NaI detector, 2%~10% for GeLi detector in the activation method, the errors are adjusted, they are listed in Table 1 at column "error". Then, the average value with weight for the cross section of ^{197}Au(n,2n)^{196}Au at 14.7 MeV using their adjusted data was got:

$$\sigma=2131\pm13 \text{ mb}$$

However, the error is just the called "internal error", only reflects the statistical one in the measurements, it should be adjusted. The scale factor method was adopted for present work

$$\varepsilon^2=\frac{1}{N-1}\chi^2_{N-1}$$

Where ε denotes scale factor, N denotes the number of measurements and χ^2_{N-1} is χ square and equal to 217.0 based on the chosen measured data listed in Table 1. The adjusted error is 13 mb×ε, called "external error" and equal to 38 mb. So the evaluated value for the cross section of ^{197}Au(n, 2n)^{196}Au at neutron energy of 14.7 MeV is

$$\sigma=2131\pm38 \text{ mb}$$

Based on the late evaluation value, Yu Baosheng's, 2133±34 mb, the new measurement data after this evaluation have been collected, listed in Table 1 at column 21, 31,33, and 34 (from 1990 to 1997). According to the Bayesian method, the new evaluated value is

$$\sigma=2130.8\pm32.6 \text{ mb}$$

This result is in good agreement with our evaluated value.

2 The Recommendation for Cross Section

The data processing and fitting are carried out for present work in the following three steps:

(1) Curve fitting for the cross section data in the energy range from threshold to 30 MeV by using the least square method;

(2) Normalization of the obtained fitted curve to the evaluated cross section value at 14.7 MeV.

Fig. 3 gives the recommendation cross section of ^{197}Au(n, 2n)^{196}Au in the neutron energy range from 8.12 to 30 MeV. The recommendation results are compared with the measurements, YU Baosheng's evaluation and ENDF/B-6. It is clear that the recommended results are in agreement with the experimental data.

From Fig. 3, we found our recommendation is in good agreement with the measured data in the neutron energy range from 8.12 MeV to 30 MeV, and is lower than ENDF/B-6 in the energy range from 14.7 MeV to 30 MeV and YU Baosheng's evaluation in the energy range from 8.12 MeV to 14.7 MeV

Fig. 4 gives the comparison with the experimental data, YU Baosheng's evaluation and ENDF/B-6 in the neutron energy range of 14 to 15 MeV. It is clear that our results is very closed to YU Baosheng's evaluation and lower than ENDF/B-6, in good agreement with measurement data.

3 Summary

In present work, the results of evaluations reported by YUAN Hanrong et al. ZHAO Wenrong et al., Jose Martinez-Rico and YU Baosheng et al. are compared. The experimental data were collected, evaluated and adjusted for neutron energy, standard cross section, and gamma branching and the cross section of ^{197}Au(n, 2n)^{196}Au at the energy 14.7 MeV was evaluated, the evaluation value is 2131±38 mb. The recommendation cross section of ^{197}Au(n,2n) ^{196}Au in the neutron energy range from 8.12 to 30 MeV and comparisons with measured data, ENDF/B-6 and YU Baosheng's evaluation, were carried out.

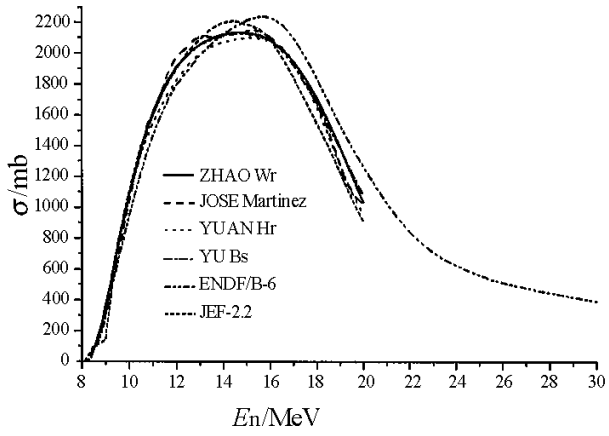

Fig.1 Comparison of the several differential evaluation results

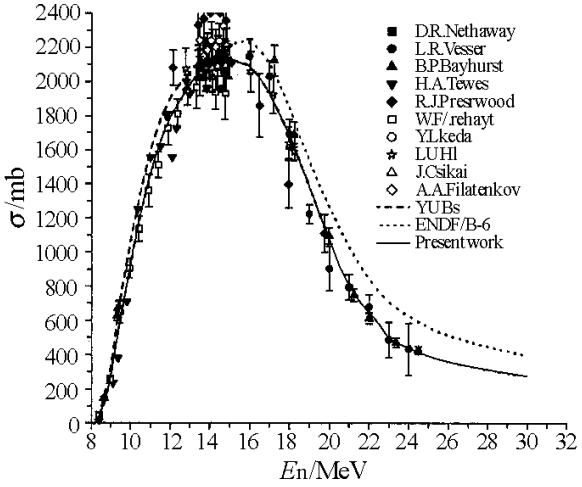

Fig.3 The recommendated cross section of ^{197}Au(n,2n)^{196}Au and the comparison with Yu Baosheng's evaluation and ENDF/B-6

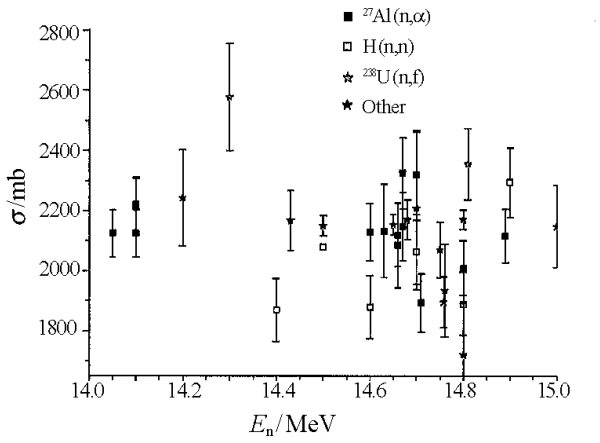

Fig. 2 Comparison of the four groups of experimental data with different standards

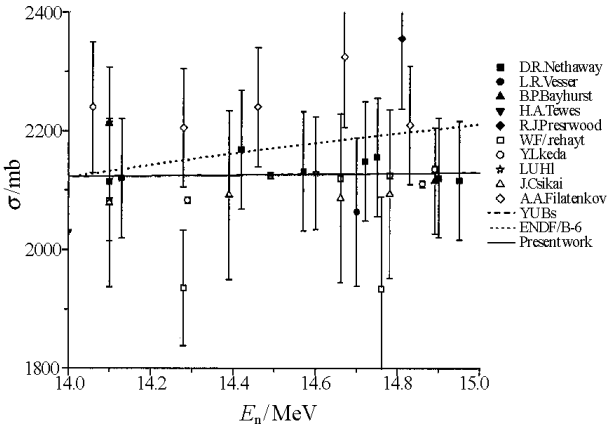

Fig.4 Comparison of cross section of ^{197}Au(n,2n)^{196}Au with experimental data, YU Baosheng's evaluation and ENDF/B-6 in the energy range of 14 to 15 MeV

References

[1] YUAN Hanrong et al. INDC(CPR)-027/L, 7, 53 (1992)

[2] ZHAO Wenrong et al. INDC(CPR)-16 (1989)

[3] Jose Martinez-Rico, INDC(NDS)-285 (1993)

[4] YU Baosheng et al. INDC(CPR),12,54(1994)

[5] T B Ryves et al. EUR-11912-EN(1989)

[6] R.C.BARRALL et al. AFWL-TR-68-134(1969)

[7] A.K.HANKLA et al. Nucl.Phys., A180,157(1972)

[8] D.R.NETHAWAY, Nucl. Phys., A190,635(1972)

[9] L.R.VEESE et al. Phys. Rev.,C,16,1792(1977)

[10] B.P.BAYHURST et al. Phys. Rev., C,12,451,(1975)

[11] H.A.TEWES et al. UCRL-6028-T,(1960)

[12] R.J.PRESTWOOD et al. Phys. Rev., 121,1438(1961)

[13] L.R.GREENWOOD, ASTM-STP-956,743(1987)

[14] J. FREHAUT, CEA-R-4627(1974)

[15] A.PAULSEN et al. NEANDC(E)-161,207(1974)

[16] S.M.QAIM, Nucl. Phys., A,185,614(1972)

[17] D.S.MATHER et al. AWRE-O-72/72,(1972)

[18] W.DILG et al. Nucl. Phys. A,118,9(1968)

[19] P.ANDERSSON et al. LUNF-D6-3021(1978)
[20] J.LAUREC et al. CEA-R-5109(1981)
[21] T.B.RYVES et al. J. Phys. ,G,7,(1),115(1981)
[22] Y.IKEDA et al. EXFOR Data No. 21945005
[23] Y.IKEDA et al. JAERI-1312(1988)
[24] K.KOBAYASHI et al. EXFOR Data No. 22093001
[25] I.KIMURAet al. Nucl. Sci. and Eng.,106,332(1990)
[26] D.MAOR et al. Phys. Rev., C,6,315(1972)
[27] J.CSIKAI, EXFOR Data No.30640001
[28] A.REGGOUG et al. EXFOR Data No. 30698001
[29] M.HERMA et al. EXFOR Data No.30803001
[30] I.GARLEA et al. INDC(ROM)-15,(1983)
[31] WANG XIUYUAN et al. EXFOR Data No.30935001
[32] S.K.MANGAL et al. NP,69,158,(1965)
[33] I.GARLEA et al. RRP,37,(1),19(1992)
[34] G.N.MASLOV et al. YK-9,50(1972)
[35] A.A.FILATENKOV et al. RI-252(1999)

The Effect of the Decay Data on Activation Cross Section

HUANG Xiaolong
China Nuclear Data Center, Beijing 102413

【**abstract**】*The effect of the decay data on evaluation of activation cross section is investigated. Present work shows that these effects must be considered carefully when activation cross section is evaluated. Sometime they are main reason for causing the discrepancies among the experimental data.*

Introduction

The neutron activation cross sections are very useful in nuclear engineering applications especially in fission and fusion reactors, and nuclear physics studies. They are also used to confirm predictions of nuclear reaction theory. As developing of nuclear technology and nuclear engineering, more accurate evaluated data are required.

Up to now, a lot of neutron activation cross sections have been measured by activation method. And there are large discrepancies among some reactions.

There are many factors, which affects the accuracy of the experimental data. According to the principle of activation method, the decay data of product is one of the factors which will affect the measured data. In order to provide more reliable and accurate evaluated nuclear data, evaluation is necessary for decay data.

In this work, the effect of the decay data on activation cross section is investigated. Some examples are given to show these effects.

1 The Effect of Decay Data

According to the principle of activation method, the decay data of residual nucleus will affect the result of measured data. Usually the decay data include the half-life of the residual nucleus, γ branching ratio of the residual nucleus. On the other hand, the decay scheme of the product will play an important role in selecting the γ rays which were used to determine the radioactivity of the reaction products.

In the following paragraph, the effect of the decay data will be discussed briefly.

1.1 Half-life

Generally speaking, the half-life of the residual nucleus doesn't cause the large discrepancies among the measured data. But the value of half-life changed largely, it will cause the conflict among the measured data. Sometime this is a main reason for the discrepancies.

Here we selected the ^{109}Ag(n,2n)^{108m}Ag reaction as an example, showing in Fig. 1. Obviously the measured data can be divided into two groups. The experimental data measured by half-life of 127 year before 1993 are much lower than those of 418 year after 1993. We investigated the experimental conditions carefully and found that the half-life was the main reason for causing the discrepancies. If the experimental data were rough adjusted by

$$\sigma_{new} = \sigma_{old} T_{1/2}^{new} / T_{1/2}^{old} \quad (1)$$

the experimental data measured by half-life of 127 years would be in agreement with those of 418 years (see Table 1 in detail).

Table 1 Comparison of the measurements for ^{109}Ag(n,2n) ^{108m}Ag reaction with different $T_{1/2}$

E_n/MeV	$T_{1/2}$(127 a)		
	Wang92[1] (mb)	Ikeda91[2] (mb)	Csikai91[3] (mb)
13.64	223		
13.79	223		
14.03	227		
14.33	224		
14.5			263
14.6	232		
14.8	236	191	

E_n/MeV	$T_{1/2}$(418 a)		
	Wang92 (mb)	Ikeda91 (mb)	Csikai91 (mb)
13.64	759/734*		
13.79	759/734*		
14.03	774/747*		
14.33	763/737*		
14.5			716/865*
14.6	790/764*		
14.8	805/777*	671/629*	

* Adjusted measurements by Eq.(1).

1.2 γ Branching Ratio

The collected experimental data will be normalized with the newest γ branching ratio by evaluators firstly when evaluating the activation cross sections. This is because the value of the measured data will be changed when the new γ branching ratio is different from the old one. Of course this is the advantage of the activation method.

Usually the corrected factor is calculated by

$$\sigma_{new} = \sigma_{exp} I_{\gamma,old} / I_{\gamma,new} \quad (2)$$

where σ_{new} and $\sigma_{exp.}$ is the adjusted cross section and measured cross section, respectively. I_γ is the branching ratio of measured gamma ray.

Sometime the effect of γ branching ratio on measured data is very large. A typical example is the ^{187}Re(n,2n)^{186g}Re reaction, as shown in Fig. 2. For the ^{187}Re(n,2n)^{186g}Re reaction, the experimental data of FAN Tieshuan et al.[16] are obviously higher than other measurements. The I_γ value of 137 keV γ ray they used is 8.5%, which is much lower than the newest value, 9.22%[17]. After normalized with the new value, their measurements are in agreement with other measured data within the error.

1.3 Decay Scheme

The ^{181}Ta(n,2n)^{180g}Ta reaction (see Fig. 3 in detail) will be an example to show the effect of the decay scheme on activation cross sections.

In the energy range above 12 MeV, the available data can be divided into two groups according to their values. The data of ZHAO Wenrong et al.[22] are higher than that of R. J. Prestwood et al.[18] and M. Bormann et al[19]. These discrepancies were caused by using different decay scheme. The different decay scheme and relevant parameters of the product ^{180g}Ta is listed in Table 2. The decay scheme of the product ^{180g}Ta is shown in Fig. 4.

Table 2 Different decay schemes and data for ^{180g}Ta product

	Brown[25]	Gallagher[26]	Ryves[24]
a/%	11	3.2	3.5
b/%	10	9.8	14.6
c/%	79	27	24.3
d/%		60	57.6
I_γ(E_γ=93 keV)		4.682	4.274
I_γ(E_γ=104 keV)		0.715	0.793

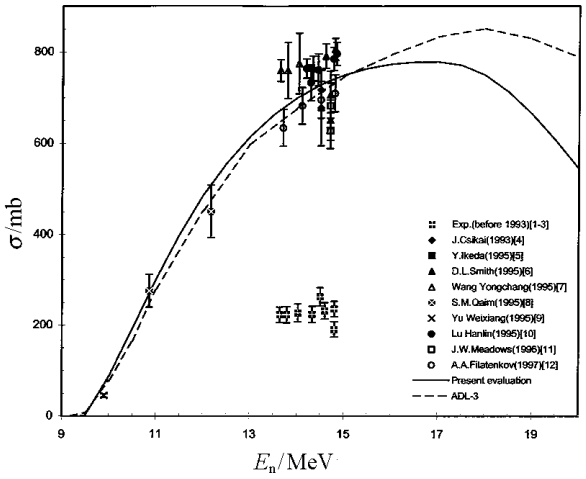

Fig.1 The cross section for ^{109}Ag(n,2n) ^{108m}Ag reaction

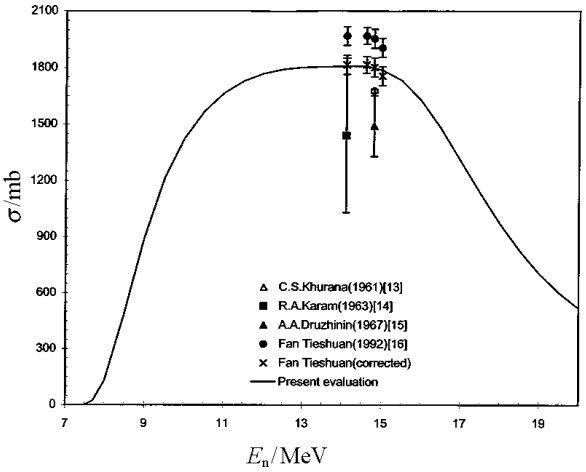

Fig.2 The cross section for ^{187}Re(n,2n) ^{186g}Re reaction

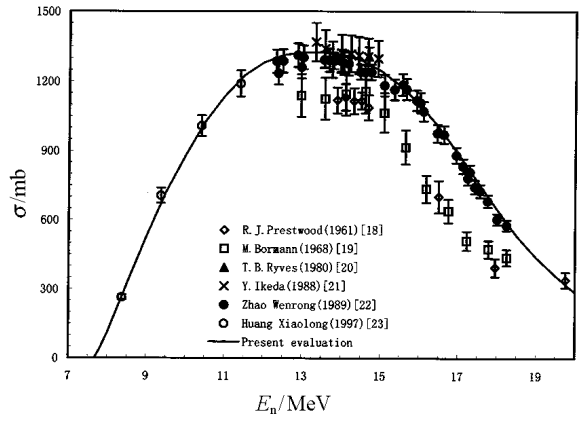

Fig.3 The cross section for ^{181}Ta(n,2n) ^{180g}Ta reaction

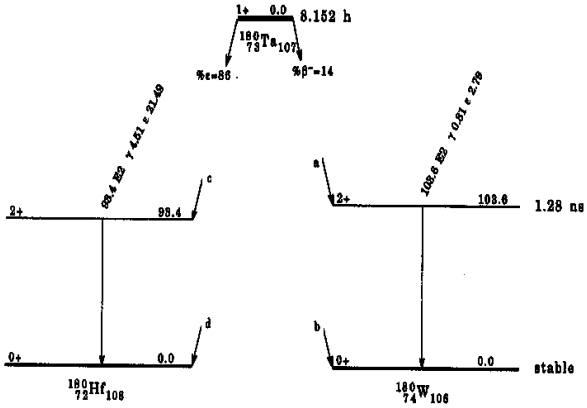

Fig.4 Decay scheme of ^{180g}Ta

In order to check the effect of decay scheme on activation cross sections, the results measured by Zhao, Prestwood, Bormann and Ryves were deduced and discrimined at 14.5 MeV with different decay schemes (see Table 3 in detail).

Tbale 3 Comparison of the ^{181}Ta(n,2n)^{180g}Ta cross section deduced with different decay schemes at 14.5 MeV

Author	Brown[25] (mb)	Gallagher[26] (mb)	Ryves[24] (mb)	Method
Prestwood[18]	1116	1802	1288	β
Bormann[19]	1157	1869	1335	β
Ryves[20]		1178	1307	γ(93 keV)
ZHAO[22]		1351	1269	γ(93+104 keV)

It's obvious that good agreement was obtained among these measurements after normalization with decay scheme of Ryves.

This example shows that the effect of decay scheme on activation cross sections is very large. And this effect must be considered carefully when evaluated.

2 Conclusions

The effect of the decay data on activation cross section is investigated carefully and testified by several examples. These decay data include the half-life, γ branching ratio of the product and its decay scheme.

Present work shows that these effects must be considered carefully when evaluating the activation cross section. Sometime they are main reason for causing the discrepancies among the experimental data.

References

[1] WANG Rongchang et al. High energy and nuclear phys. 16, 731(1992).
[2] Y.Ikeda et al. JAERI-M-91-032, 272, 1991.
[3] J.Csikai et al. Ann. Nucl. Energy 18, 1(1991).
[4] J.Csikai et al. INDC(NDS)-286, 1993.
[5] Y.Ikeda et al. INDC(NDS)-342, 19(1995).
[6] D.L.Smith et al. INDC(NDS)-342, 7(1995).
[7] WANG Yongchang et al. INDC(NDS)-342, 37 (1995).
[8] S.M.Qaim et al. INDC(NDS)-342, 47(1995).
[9] YU Weixiang et al. INDC(NDS)-342, 41(1995).
[10] LU Hanlin et al. INDC(NDS)-342, 37(1995).
[11] J.W.Meadows et al. Ann. Nucl. Energy, 23, 877(1996).
[12] A.A.Filatenkov et al. INDC(CCP)-402, 1997.
[13] C.S.Khurana et al. Nucl. Phys., 28, 560(1961).
[14] R.A.Karam et al. AD-402668, 1963.
[15] A.A.Druzhinin et al. Report YF-5, 18, 1967.
[16] Fan Tieshuan et al. Chinese J Nucl. Phys., 14, 331 (1992).
[17] C.M.Baglin, Nucl.Data Sheets, 82, 1 (1997)
[18] R.J.Prestwood et al. Phys. Rev., 121, 1438(1961).
[19] M.Bormann et al. Nucl. Phys., A115, 309(1968).
[20] T.B.Ryves et al. J of Phys. G, 6, 771(1980).
[21] Y.Ikeda et al. JAERI-1312,1988.
[22] ZHAO Wenrong et al. INDC(CPR)-16, 1989.
[23] HUANG Xiaolong et al. INDC(CPR)-045, 1998.
[24] T.B.Ryves et al. J. Phys. G6, 763(1980).
[25] H.N.Brown et al. Phys. Rev. 84, 292(1951).
[26] C.J.Gallagher et al. Nucl. Phys. 33, 285(1962).

A Testing of RIPL with UNF Code Calculation in Energy Region 0.1~20 MeV

GE Zhigang ZHANG Jingshang SUN Zhengjun
China Nuclear Data Center, CIAE, P.O.Box 275-41, Beijing 102413
e-mail:gezg@iris.ciae.ac.cn

Introduction

For general testing and validation of the RIPL[1] database, a nuclear model code UNF[2] was used to perform the testing with RIPL database. The testing was done in the incident energy region of 0.1~20 MeV for 103 nuclei and mass region from 69 to 160.

1 The Information of Nuclei and Model Parameters

Nuclear data model calculations need two important kinds of information. One is nuclear character, including mass, spin and nuclear discrete level for the target, compound and residual nuclei. This kind of information can be obtained from the nuclear experimental measurements. Other one is the information about the nuclear reaction model code used, which contains the related model parameters. These parameters can be adjusted in a reasonable range according to the experimental data for an individual reaction calculation.

In this work all nuclear character of target, compound, residual nuclei and model parameters are taken from RIPL database.

2 The Code and Calculation

Nuclear reaction model code UNF was used in this work, which is one of main nuclear data evaluation tools in the nuclear data evaluation activities of Chinese Evaluated Nuclear Data Library (CENDL-2 and 3). 103 nuclei of the mass region from 69 to 160 were involved in this work for neutron incident energy region of 0.1~20 MeV. The calculations were performed by using all parameters taken from RIPL firstly without any adjusting. Then the necessary modifying to some parameters was introduced according to the experimental data for some reaction channels.

3 Results

As one knows that the optical potential parameters is most important for the total cross sections calculations, and the optical parameters collected in RIPL were obtained by fitting the experimental total cross sections and elastic scattering angular distributions. The calculated total cross sections with the parameters are in very good agreement with the experimental total cross sections (the errors are less than 3%).

As examples, in Fig.1 to Fig. 9 are presented the UNF calculated results with and without model parameter modifying for other main reaction channels, for instance, (n,gamma), (n,2n) and (n,3n),et al. One can see that the calculated results without the parameter modifying could repeated the behavior of most the experimental data in physical shape, except for the absolute value for these reaction channels. When some necessary adjusting for model parameters of the RIPL according to the related experimental data were introduced, the calculated results could reproduce the experimental data well.

4 Conclusions

Through the comparisons of the calculations, following conclusions in this energy and mass region can be obtained: (a) RIPL database covered the most of the information and parameters for nuclear study, nuclear data model calculations and its applications. (b) The data concerning nuclear characters are latest and accurate. (c) The related model parameters are reasonable in physics and acceptable for nuclear data model calculations in energy 0.1～20 MeV. (d) Some model parameter adjusting is necessary based on the related experimental information.

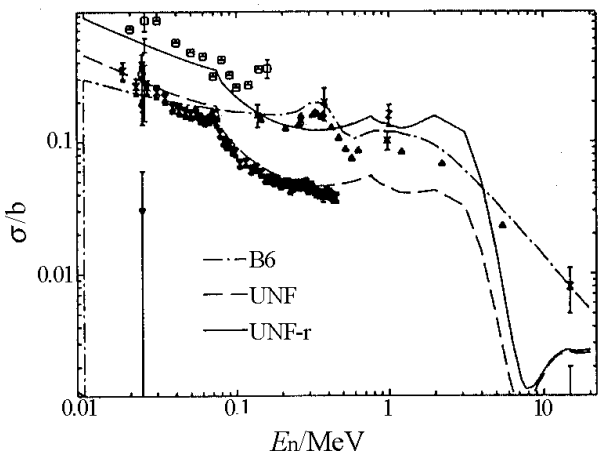

Fig.1 Comparison of (n,γ) cross sections among the calculated results with (full line) ,without (dashed line) parameter modifying and ENDF/B-6 (dot-dashed line) and experimental data for ^{164}Dy

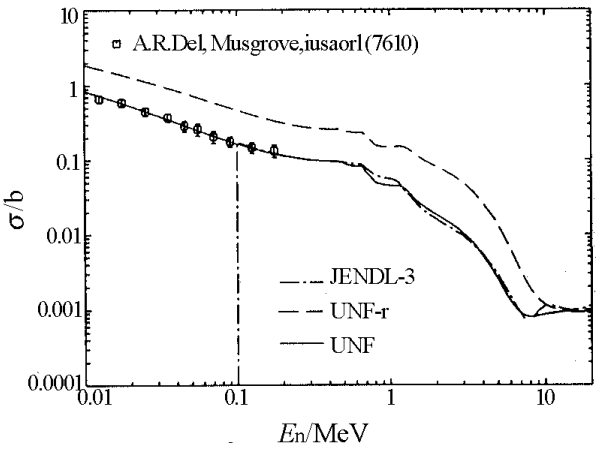

Fig.2 Comparison of (n,γ) cross sections among the calculated results with (full line) ,without (dashed line) parameter modifying and JENDL-3 (dot-dashed line) experimental data for ^{97}Mo

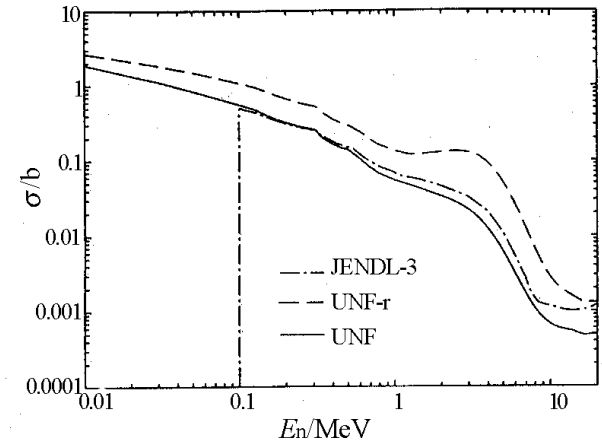

Fig.3 Comparison of (n,γ) cross sections among the calculated results with (full line), without (dashed line) parameter modifying and JENDL-3 (dot-dashed line) for ^{101}Ru

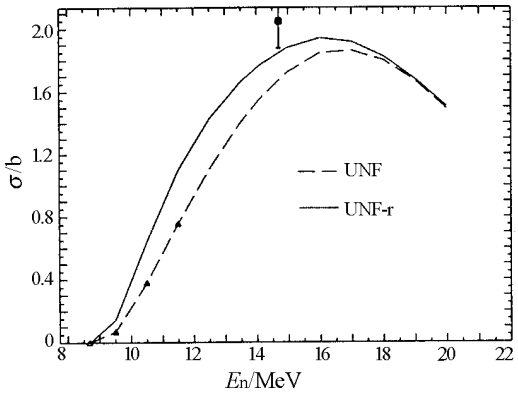

Fig.4 Comparison of (n,2n) cross sections among the calculated results with (full line) and without (dashed line) parameter modifying and experimental data for ^{153}Eu

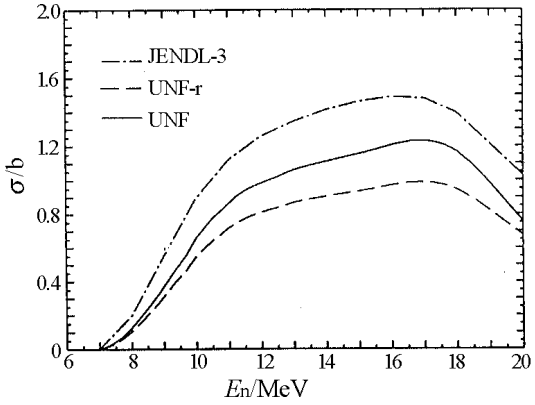

Fig.5 Comparison of (n,2n) cross sections among the calculated results with (full line), without (dashed line) parameter modifying and JENDL-3 (dot-dashed line) for ^{97}Mo

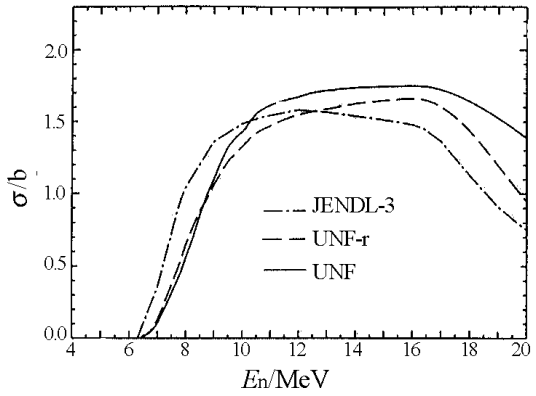

Fig.6 Comparison of (n,2n) cross sections among the calculated results with (full line), without (dashed line) parameter modifying and JENDL-3 (dot-dashed line) for ^{103}Ru

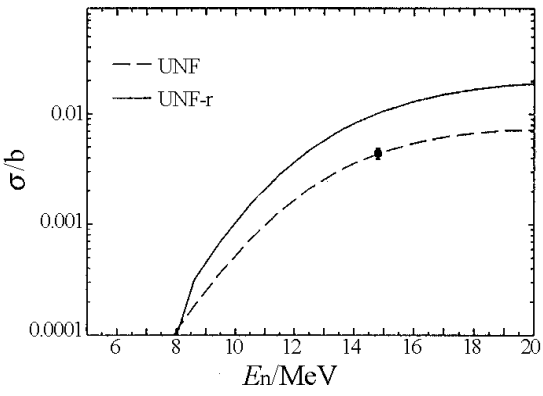

Fig.7 Comparison of (n,p) cross sections among the calculated results with (dashed line) and without (full line) parameter modifying and experimental data for ^{153}Eu

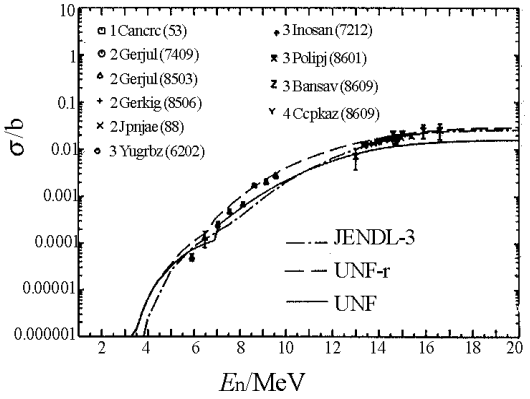

Fig.8 Comparison of (n,p) cross sections among the calculated results with (full line), without (dashed line) parameter modifying and JENDL-3 (dot-dashed line) and experimental data for ^{97}Mo

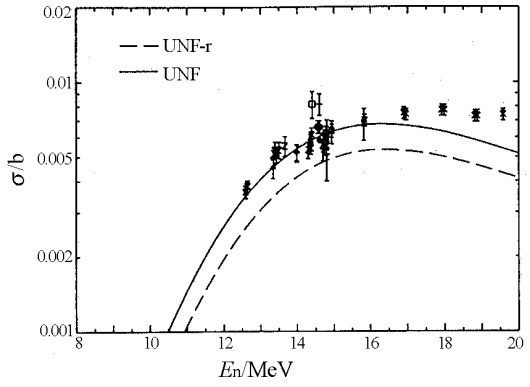

Fig.9 Comparison of (n,α) cross sections among the calculated results with (full line), without (dashed line) parameter modifying and experimental data for ^{98}Mo

Reference

[1] Oblozinsky. P. Handbook for calculations of nuclear reaction data, Reference input parameter library, IAEA-TECDOC-1034, (1998).

[2] ZHANG Jingshang. User Manual of UNF Code, CNIC-01616.

A Comparison of Two Level Density Models in Energy Region 0~20 MeV

GE Zhigang, SUN Zhengjun

China Nuclear Data Center, CIAE, P.O.Box 275-41, Beijing 102413

e-mail: gezg@iris.ciae.ac.cn

Introduction

The Gilbert-Cameron (G-C) and Back-Shift (B-S) level density approaches are widely used in the nuclear reaction data model calculations in incident energy less than 20 MeV. Some sets of the level density parameters for the G-C and B-S approaches have been recommended and selected by the Reference Input Parameter Library (RIPL) Starter File[1]. To give a brief view about these parameters, the basic testing for these parameters is necessary. This work presents the comparison of the cumulative number of levels calculated by using G-C and B-S models with the related parameters recommended by RIPL and the experimental ones recommend by G. L. Molnar et al.[1] for 303 nuclei. The comparison of the calculated D_0 and experimental D_0 recommended by Beijing group[1] also performed in this work.

1 G-C and B-S models and Calculations

The composite Gilbert-Cameron formula[2] reads as follows:

$$\rho(E)=\begin{cases}\dfrac{1}{T}\exp(E-E_0/T) & E\le E_x\\ \dfrac{1}{12\sqrt{2}\sigma a^{1/4}(E-\Delta)^{5/4}}\exp\left(2\sqrt{a(E-\Delta)}\right) & E\le E_x\end{cases}$$

where α is the level density parameter, and σ^2 is the spin cutoff parameter, which are determined by the relations

$$\sigma^2=0.0888(a(E-\Delta))^{1/2}A^{2/3}$$

$$\frac{a}{A}=0.00917((S(Z)+S(N))+Q(Z,N)$$

where *S(Z)*, *S(N)* are the shell corrections for protons and neutrons, respectively, and *Q(Z,N)* =0.142 for 54<*Z*<78, 86<*N*<122, and *Q(Z,N)*=0.120 for 86<*Z*<122, 130<*N*<182.

The Back-Shift formula [3] reads as follows:

$$\rho(E)=\frac{\exp\left(2\sqrt{a(E-\Delta)}\right)}{12\sqrt{2}\sigma a^{1/4}(E-\Delta+t)^{5/2}}$$

where Δ is the excitation energy shift. σ and t can be obtained by the following relations

$$\sigma^2=0.0073A^{5/3}$$

$$U-\Delta=at^2-t$$

The level density parameters Δ and α are most important. They are obtained by analyzing the experimental cumulative number of levels N and the s-wave average resonance spacing D_0 at neutron binding energy in a wide region of nuclei.

One can calculate the level density with the above formulae and the related level density parameters were recommended by RIPL Start File, and the cumulative number of levels can be obtained by following relation

$$N(E)=\int_0^E\rho(E)\mathrm{d}E$$

The average resonance spacing D_0 can be obtained from the cumulative number of levels at neutron binding energy E_n by a simple relation

$$D_0 = \frac{1}{\rho(E_n, J, \pi)}$$

Considering the nuclide region of the recommended parameters for G-C and B-S formulae, 303 nuclei (from ^{24}Na to ^{250}Cf) were selected for the calculations. The cumulative number of levels and D_0 of these nuclides in the energy region of 0~20 MeV were calculated with the G-C and B-S models. Because the level density parameters used in the calculations were recommended by the Beijing group, so the experimental values of D_0 recommended by Beijing group were used in the comparisons.

2 Results

As examples, Fig. 1 presents some comparison of the calculated D_0 by G-C and B-S level density model with experimental ones for 303 nuclides. One can see that the most calculated results are acceptable although there are some deviation for some nuclei.

In Fig. 2 are shown the comparisons of the experimental cumulative number of levels, recommend by G. L. Molnar et al.[1], with calculated ones for some nuclides. The full line represents the cumulative number of levels recommended by G. L. Molnar et al. The dashed line and dot-dashed line correspond to the results calculated by G-C and B-S models, respectively. In general, both of the G-C and B-S models and related parameters recommended by RIPL Start File can reproduce the experimental value well. In some cases the behaviors of the G-C are better than the B-S, but worse for others. About 3% of the calculations of the G-C and B-S are very far from the experimental values.

3 Conclusion

From the calculations of the cumulative number of levels N and average resonance spacing D_0 with G-C and B-S level density models, and the comparison with related experimental values in this work, it is concluded that G-C and B-S level density models and related parameters recommended by RIPL Start File are reasonable in the energy region of 0~20 MeV and mass region from ^{24}Na to ^{250}Cf.

References

[1] Handbook for Calculations of Nuclear Reaction Data, Reference Input Parameter Library, IAEA-TECDOC-1034, (1998).

[2] A.Gilbert, C.G.W. Cameron. Con. J.Phys., 43, 1446 (1965).

[3] W. Dilg et al. Nucl. Phys., A217, 485(1975).

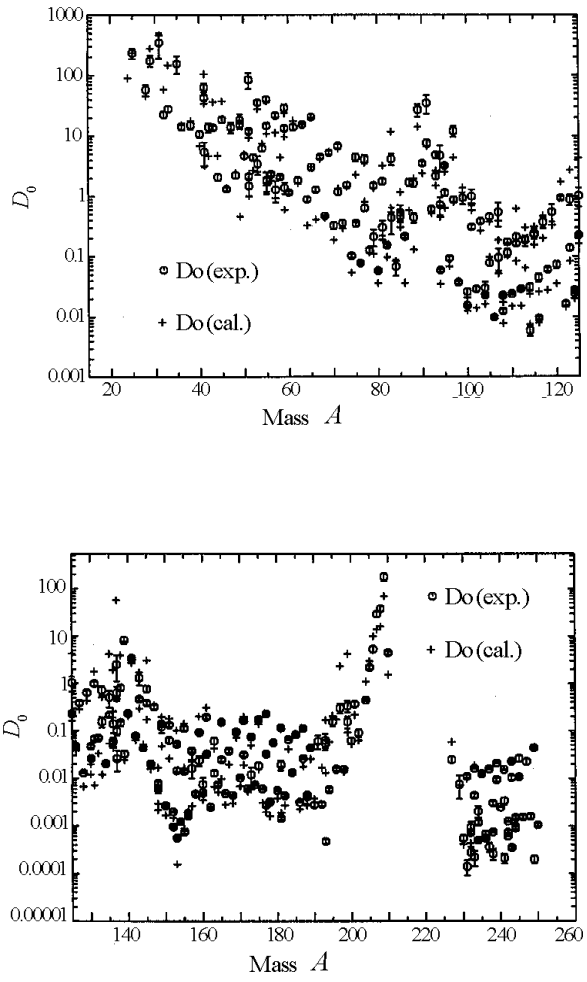

Fig. 1 Comparison of the calculated D_0 by G-C and B-S level density model with experimental ones for 303 nuclides

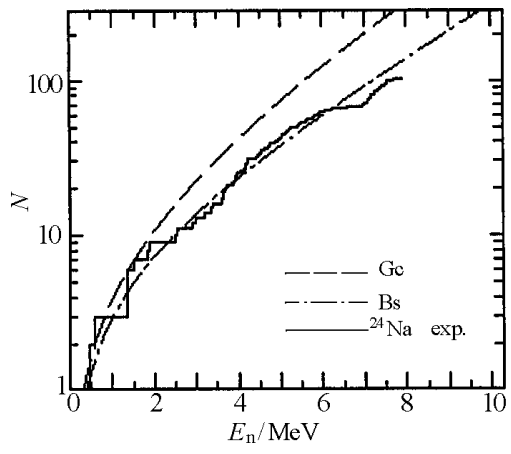

(a)

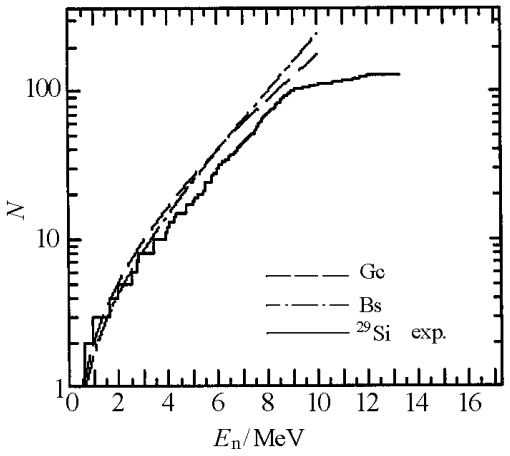

(d)

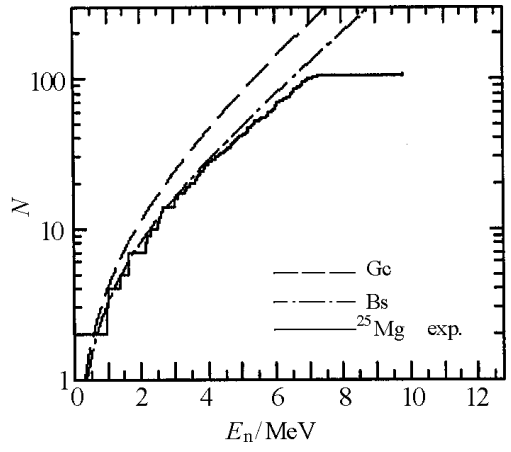

(b)

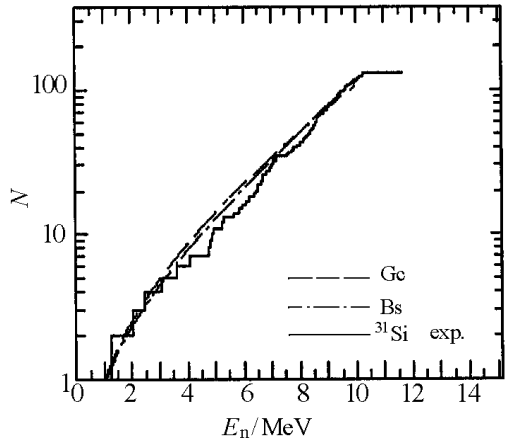

(e)

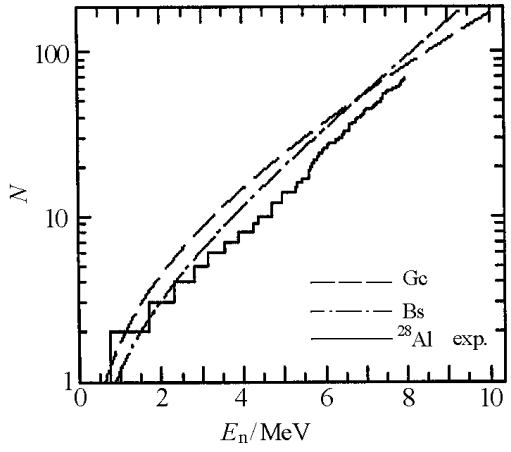

(c)

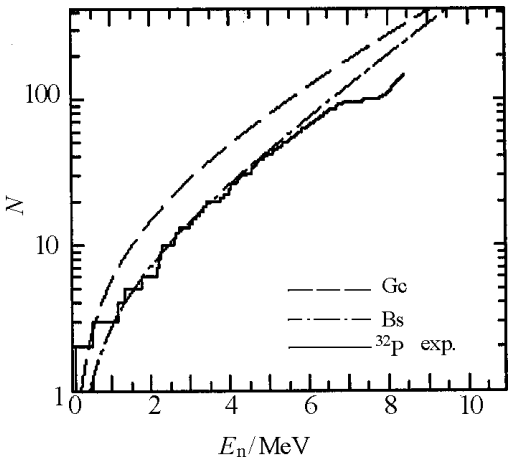

(f)

Fig.2 Comparison of the calculated cumulative number of levxz els and the experimental one recommend by G. L. Molnar et al

Activities and Cooperation in Nuclear Data Field in China during 2001

ZHUANG Youxiang

China Nuclear Data Center, CIAE, Beijing

e-mail: yxzhuang@iris.ciae.ac.cn

1 Meetings Held in China

(1) The meeting on the 10th five year plan of nuclear data evaluation, June 12~17, Zhangjiajie city, Hunan province;

(2) The Working Group Meeting of Nuclear Data Evaluation and Theoretical Calculation, July 25, Beijing;

(3) The Standing Committee Meeting of the Second China Nuclear Data Committee, Sep. 13, Beijing;

(4) The plenary session of the China Nuclear Data Committee, Sep. 14, Beijing,

Prof. ZHAO Zhixiang, president of CIAE, was appointed to be the new chairman of the committee.

2 The International Meetings in Nuclear Data Field Attended by Staffs of CNDC

(1) Research Co-ordination Meeting on Development of a Data base for Prompt Gamma-ray Neutron Activation Analysis, May 14~17, ZHOU Chunmei, Vienna, Austria;

(2) Consultants' Meeting on the Co-ordination of Nuclear Reaction Data Centers (Technical Aspects), May 28~31, ZHUANG Youxiang, Vienna, Austria;

(3) International Conference on Nuclear Data for Science and Technology, Oct. 7~12, XIA Haihong, ZHUANG Youxiang, ZHOU Zuying, YU Weixiang, SHEN Qingbiao and YU Hongwei, Tsukuba, Japan;

(4) Research Co-ordination Meeting on Fission Product Yield Data Required for Transmutation of Minor Actinide Nuclear Waste, Oct. 8~12, LIU Tingjin, Vienna, Austria;

(5) Research Co-ordination Meeting on Final Stage of WIMS-D Library Update Project, Nov. 5~8, LIU Ping, Vienna, Austria;

(6) Research Co-ordination Meeting on Nuclear Model Parameter Testing for Nuclear Data Evaluation (Reference Input Parameter Library: Phase II), Dec. 3~7, GE Zhigang, Vienna, Austria.

3 The Foreign Scientists in Nuclear Data Field Visited CNDC/CIAE

(1) Drs. T.V.Golashvili, V.P.Chechev and A.Demidov, Ministry of Atomic Energy of Russia Federation, Sep. 10~20;

(2) Dr. Jun-ichi Katakura, NDC/JAERI, Sep. 16~21;

(3) Dr.Guinyun Kim, Pohang Technology University, Korea, Sep. 20~21;

(4) Dr. Andrej Trkov, NDS/IAEA, Oct. 13~17;

(5) Dr. E.T.Cheng, San Diego, USA, Nov. 16.

4 Staffs of CNDC Worked in or Visited Foreign Country

(1) RONG Jian, JAERI, from Aug. 1, 2000 to July 31, 2001;

(2) SHU Nangchuan, ORNL, from Mar. 26, 1999 to Oct. 1, 2

CINDA INDEX

Nuclide	Quantity	Energy/ eV		Lab	Type	Documentation				Author, Comments
		Min	Max			Ref	Vol	Page	Date	
^{6}Li	(n,t)	1.8+6	2.7+6	BJG	Expt	Jour CNDP	27	1	Jan 2002	ZHANG Guohui +, DDX, CS, TBL, IOCH
^{112}Sn	Calculation	1.0+3	2.0+7	UNW	Theo	Jour CNDP	27	9	Jan 2002	DUAN Junfeng +, SIG, DA, DE
^{120}Sn	Calculation	1.0+3	2.0+7	UNW	Theo	Jour CNDP	27	9	Jan 2002	DUAN Junfeng +, SIG, DA, DE
^{197}Au	(n,2n)	1.4+7		SIU	Expt	Jour CNDP	27	4	Jan 2002	MOU Yunfeng +, SIG,HPGe
	(n,2n)	Thrsh	3.0+7	AEP	Eval	Jour CNDP	27	19	Jan 2002	FAN Sheng, SIG
^{239}Pu	Prompt Neuts	1.0-5	2.0+7	AEP	Eval	Jour CNDP	27	14	Jan 2002	YU Baosheng +, YLD
	Delayed Neuts	1.0-5	2.0+7	AEP	Eval	Jour CNDP	27	14	Jan 2002	YU Baosheng +, YLD